

UC Berkeley

UC Berkeley Previously Published Works

Title

Quantitative elemental imaging in eukaryotic algae

Permalink

<https://escholarship.org/uc/item/34d9n16x>

Journal

Metallomics, 15(5)

ISSN

1756-5901

Authors

Schmollinger, Stefan

Chen, Si

Merchant, Sabeeha S

Publication Date

2023-05-02

DOI

10.1093/mtomcs/mfad025

Copyright Information

This work is made available under the terms of a Creative Commons Attribution License, available at <https://creativecommons.org/licenses/by/4.0/>

Peer reviewed

Synchrotron-based Imaging Strategies to Visualize (trace) Metals

Quantitative elemental imaging in eukaryotic algae

Stefan Schmollinger ^{1,2,*}, Si Chen ³ and Sabeeha S. Merchant ^{1,2}

¹California Institute for Quantitative Biosciences (QB3), University of California, Berkeley, CA 94720, USA, ²Departments of Molecular and Cell Biology and Plant and Microbial Biology, University of California, Berkeley, CA 94720, USA and ³X-ray Science Division, Argonne National Laboratory, Lemont, IL 60439, USA

*Correspondence: MSU-DOE Plant Research Laboratory, Michigan State University, 612 Wilson Road, East Lansing, MI 48824, USA. Tel: +1 (310) 779-0687; Email: schmolli@msu.edu

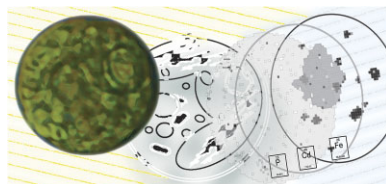
[†]Present address: MSU-DOE Plant Research Laboratory, Michigan State University, East Lansing, MI 48824, USA

Abstract

All organisms, fundamentally, are made from the same raw material, namely the elements of the periodic table. Biochemical diversity is achieved by how these elements are utilized, for what purpose, and in which physical location. Determining elemental distributions, especially those of trace elements that facilitate metabolism as cofactors in the active centers of essential enzymes, can determine the state of metabolism, the nutritional status, or the developmental stage of an organism. Photosynthetic eukaryotes, especially algae, are excellent subjects for quantitative analysis of elemental distribution. These microbes utilize unique metabolic pathways that require various trace nutrients at their core to enable their operation. Photosynthetic microbes also have important environmental roles as primary producers in habitats with limited nutrient supplies or toxin contaminations. Accordingly, photosynthetic eukaryotes are of great interest for biotechnological exploitation, carbon sequestration, and bioremediation, with many of the applications involving various trace elements and consequently affecting their quota and intracellular distribution. A number of diverse applications were developed for elemental imaging, allowing subcellular resolution, with X-ray fluorescence microscopy (XFM, XRF) being at the forefront, enabling quantitative descriptions of intact cells in a non-destructive method. This Tutorial Review summarizes the workflow of a quantitative, single-cell elemental distribution analysis of a eukaryotic alga using XFM.

Keywords: heavy metal detoxification, iron, copper, XRF, SXRF, Chlamydomonas

Graphical abstract



Elemental imaging of a single-celled eukaryotic alga using X-ray fluorescence.

The aim of this review is to (1) highlight the contributions of different elements to photosynthetic life and the concepts of how organisms control their elemental composition, (2) introduce the methodologies involved in studying elemental distributions in cells, especially XFM, (3) review the current state of XFM studies in eukaryotic algae, and (4) extract a methodology framework for conducting XFM studies from these works. It is our goal to facilitate the entry into the field of elemental research for algae scholars encountering questions of metal homeostasis and elemental heterogeneity for the first time, and to encourage the use of quantitative elemental imaging approaches for the purpose of determining biological function.

Elemental composition of cells

The elements of the periodic table are the indivisible foundation of all matter, including all biological life on our planet (Fig. 1). Ev-

ery component of a cell is assembled from a careful selection of elements, which can either be essential to the organism, defined by their irreplaceability and absolute requirement to complete the vegetative or reproductive life cycle,¹ or provide specific beneficial advantages, improving the organism's fitness in general or in specific situations or environmental niches. The most prominent elements in living matter are C, H, N, O, P, and S, which are essential, account for most of biomass, and constitute the backbone of proteins, carbohydrates, nucleic acids, and lipids.²⁻⁴ In addition, there are many other elements that are useful to living organisms in lower abundance.¹ For example, it is estimated that ~40% of all enzymes utilize a uniquely suited element outside the group of macronutrients (CHNOPS) within their catalytic centers to enable catalysis.^{5,6} The range of essential or beneficial elements can change between different organisms depending on the organism's environmental niche and its metabolism, the latter consequently defining the organism's enzyme portfolio.

Received: August 30, 2022. Accepted: March 3, 2023

© The Author(s) 2023. Published by Oxford University Press. This is an Open Access article distributed under the terms of the Creative Commons Attribution License (<https://creativecommons.org/licenses/by/4.0/>), which permits unrestricted reuse, distribution, and reproduction in any medium, provided the original work is properly cited.

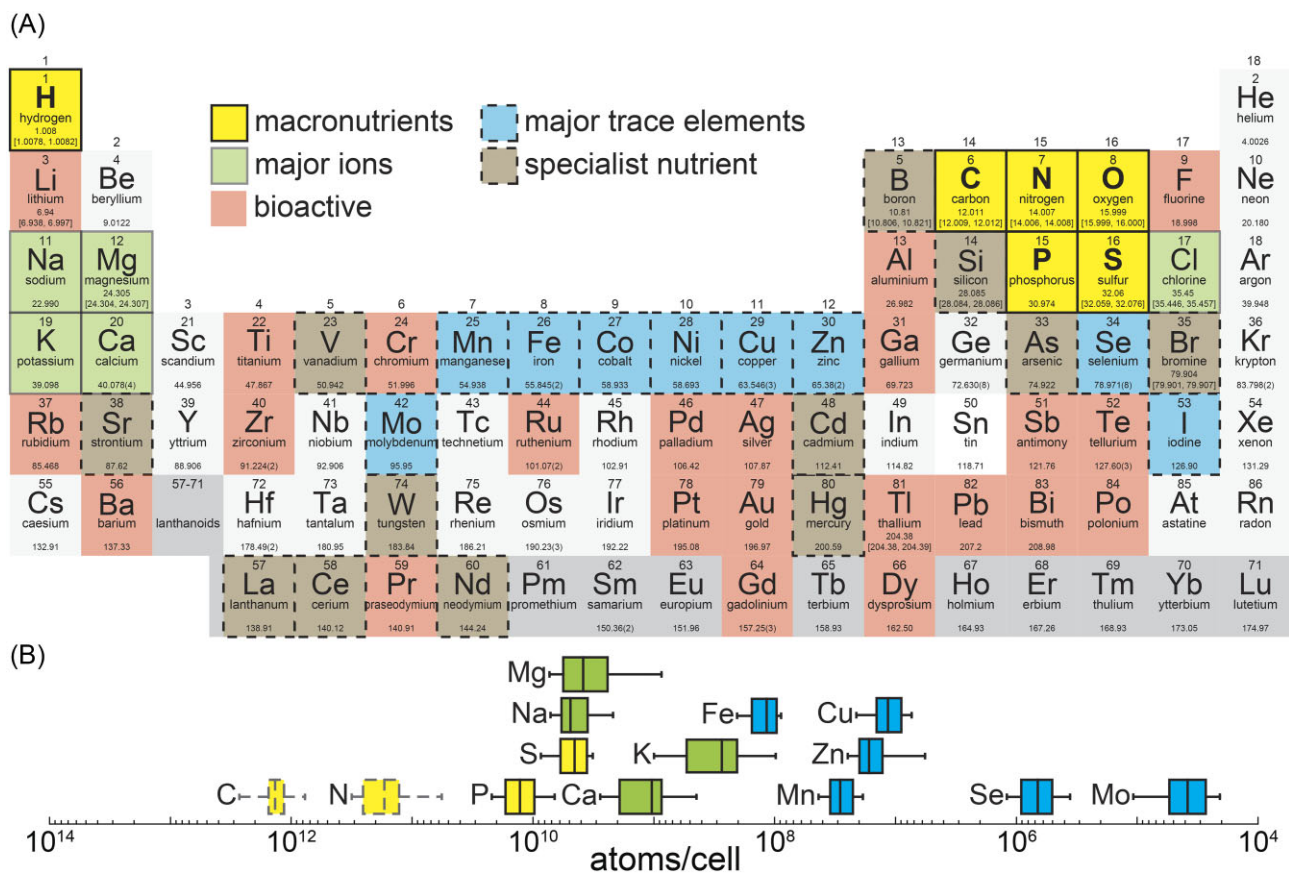


Fig. 1 Elements of interest in life. (A) Periodic table of the elements showing relevant elements to living organisms. Elements are grouped into macronutrients (CHNOPS, yellow background), the major cations (Na, Mg, K, and Ca, green background), major trace elements relevant for enzymatic function in many organisms (blue background), nutrients that are relevant for specialist's enzyme function (brown background), and elements that affect metabolism (beneficial or toxic) in living organism without being directly utilized in enzymes (bioactive, red background). (B) Elemental composition of the eukaryotic green algae *C. reinhardtii*. Solid lines indicate ICP-MS/MS analysis; dotted lines indicate TOC/TN measurements.

Most organisms use cations (K,^{7–10} Mg,^{11–15} Ca,^{16–19} and to a lesser degree Na^{20–24}) and the Cl anion,^{25–28} all of which are abundant constituents of biological matter, to regulate osmotic pressure and pH, build gradients across membranes that facilitate energy production, transport processes, or signal transduction.²⁹ These ions also serve as allosteric regulators of enzyme activity,^{9,30} even participate in catalysis (e.g. Mg in isocitrate lyase^{31,32} or Ca in the oxygen-evolving complex of PSII³³), or bind to metabolites (most importantly, Mg-ATP and Mg-chlorophyll), critically enabling their utility.

Additionally, organisms require various additional sets of elements in trace amounts (including many metal ions) to enable critical chemical functionalities that are not provided from functional groups found on metabolites or amino acids.^{4,34} These micronutrients/trace elements are often required co-factors for metabolically essential enzymes, and consequently, their acquisition, intracellular distribution, and utilization are crucial aspects of cellular metabolism.⁴ Trace elements typically present the most interesting targets for elemental imaging because of the impact of their chemistry on cell health and metabolism, the range of their abundances in an organism, and the dynamic regulation involved in their utilization.^{4,35}

A set of trace elements is essential for most organisms, including Fe,^{36–38} Cu,^{39–43} Co,^{44–47} Ni,^{48–51} Mn,^{52–55} Zn,^{56–60} Se,^{61–70} I,^{71–74} and Mo.^{75–77} Many of these elements have oxidation states that are stable under physiological conditions, and a role in redox chemistry is a common function for many of the trace el-

ements. Fe, Cu, and Mn, with multiple stable oxidation states, are therefore among the most abundant and important trace elements for all organisms; at lower abundance, Ni, Co, and Mo are also required by many organisms.^{5,36,39,44,48,52,56,75,78–80} Fe is used most famously in hemoglobin for O₂ transport, but has many other uses, e.g. in electron transport (e.g. in complex I, II, and III of the mitochondrial electron transfer chain) and as an essential catalyst in many critical enzymes (e.g. in aconitases, catalases, and nucleases), either bound directly to amino acids or alpha-ketoglutarate, complexed within the tetrapyrrole heme, or assembled into Fe-S clusters.^{81–86} Similarly, Cu can also be used for both oxygen (e.g. hemocyanin) or electron transport (e.g. cytochrome c oxidase), and can directly be bound to amino acids in catalytic centers of enzymes.^{43,87,89–91} Mn is also essential and critically involved in several enzymes in DNA metabolism, detoxification of reactive oxygen species, and carbohydrate metabolism.^{92–95} Fe, Cu, and Mn, in addition to their many important contributions to general metabolism, are also critically employed in photosynthetic electron transfer and chloroplast metabolism.^{96,97} Ni is used in enzymes in a wide range of organisms, e.g. in ureases and hydrogenases.⁹⁸ Co is utilized as a cofactor in a few enzymes directly, but is most commonly utilized at the center of cobalamin (also known as vitamin B₁₂), which is critical in methionine biosynthesis and nitrogen fixation.^{44,99,100} Mo, outside of bacterial FeMo-nitrogenase, is usually bound to the pterin cofactor Moco, which is used in many important enzymes, e.g. nitrate reductase, xanthine oxidoreductase, and sulfite oxidases.^{75,101–103} Zn is

similarly abundant and widespread as a trace element as Fe, Cu, and Mn, but is used as a Lewis acid and a structural component for proteins in most organisms.^{104–106} Se, most prominently, is utilized as selenocysteine in specific enzymes requiring the element in their catalytic centers, e.g. glutathione peroxidases.^{61,67,107–111} I is used in thyroid hormones, essential for vertebrates, and has a role in oxidative stress response in algae.^{71–74}

Other elements, V,^{67–70,110,111} B,^{112–117} Si,^{118–121} As,^{122–124} Br,^{125–127} Sr,^{128–130} Cd,^{131–134} W,^{135–139,140} Hg,^{141–143} La,^{144–147} Ce,^{148–150} and Nd,^{151, 152} are not commonly used in most organisms, but some specialists have found unique roles for these elements.^{144,146,148,151} Additionally, many of these nutrients only useful to specialist are toxic, and other, bioactive elements for which no direct enzymatic use has yet been identified (Fig. 1), can accumulate in organisms involuntarily, hijacking uptake routes for other, similar ions. They interfere with biological processes, most commonly in detrimental fashion. Together with these harmful activities associated with the redox-active trace elements (Fe, Cu, Mn, Ni, Co, and Mo), trace nutrients pose an inherent risk to cell integrity. Therefore, the chemical reactivities that make these elements useful in the first place must be controlled intracellularly to avoid unintended reactions, e.g. by using compartmentalization or detoxification mechanisms.^{153–155} The concentration of many of these elements in the direct environment of a cell is a critical parameter, determining if the organism is starving for the element as a nutrient, when either abundance or bioavailability is low, or if cell health is threatened by overexposure, exceeding demand, and the capacity for detoxification/containment.¹⁵⁶ The toxicity can either be directly attributed to detrimental reactivities of the element when uncontrolled, the production of secondary toxic products, e.g. reactive oxygen species, or enzyme/metabolite mis-metalation. Mis-metalation is largely attributed to the inherent flexibility in proteins and the similar physical properties (ionic radii, charge, and coordination preferences) of the biologically common trace metal.^{157,158} Most enzymes are tuned to function with a specific metal cofactor. Binding of a different, similar metal at the active site can result in loss-of-function, or worse, the production of unintended products or promotion of side-reactions.^{154,159,160} All organisms therefore carefully control their elemental composition at the point of uptake, resulting in specific cellular quotas, especially in the case of redox active trace elements. Cells also employ elaborate strategies to avoid mis-metalation intracellularly, including the compartmentalization of specific elements to ensure that the correct metal binds to newly synthesized proteins, or the use of metallochaperones to ensure correct delivery through protein–protein interactions.^{161–163} Some metals are associated with organic groups or build into large clusters (e.g. Fe in heme and Fe–S clusters) for similar reasons.

The pathways for trace element metabolism are among the most ancient in biology,¹⁶⁴ and the general concepts involved in trace metal utilization are well conserved across organisms. Photosynthetic organisms specifically have unique requirements with respect to the elemental composition because of the metabolic demand of the photosynthetic apparatus and the specific pressures they experience from the environmental niches they occupy. Processes realized by abundant enzymes weigh harder on the specific elemental quotas, and proteins involved in photosynthetic carbon fixation (most prominently photosystems I and II, the Cyt *b₆f* complex, and the enzymes of the Calvin–Benson cycle) are among the most abundant proteins in photosynthetic organisms. Magnesium is especially important here, with 25% of Mg in plants being found in chloroplasts, where it is integral for the

light-capturing chlorophylls (Mg-containing tetrapyrroles) and in the activation of the carbon-capturing RuBisCO.^{11,165,166} The photosynthetic electron transfer chain also requires large amounts of Fe; 80–90% of Fe in leaves is found in the chloroplast.¹⁶⁷ Most abundantly, Fe is found in photosystem I, which is utilizing three 4Fe–4S centers to transport electrons from the acceptor to the donor side, and in ferredoxin (2Fe–2S center), the soluble carrier protein distributing photosynthetically derived electrons to various chloroplast processes, including NADPH production, nitrogen assimilation, and chlorophyll biosynthesis.^{97,168} Cu in plastocyanin, the soluble electron carrier between the Cyt *b₆f* complex and photosystem I, and Mn and Ca, in the oxygen-evolving complex of photosystem II, are also vital in photosynthetic electron transport.^{17,39,169} Zn is involved in photosynthetic CO₂ fixation, in the catalytic center of carbonic anhydrases (CAHs), and in the assembly of RuBisCo.^{170,171}

Intracellular elemental heterogeneity

The elemental composition of an organism is a dynamic function of the metabolic needs of a cell. As mentioned above, it varies between organisms depending on the functions they employ, but even within a given species, it is adjusted between different metabolic or developmental stages, tissues, and cell types, and in response to the availability of nutrients and other stimuli in the environment.

Nutrient limitation is a major driver of acclimation responses to the elemental composition. While limitation to essential elements often results in cell cycle arrest or even cell death, the elemental composition of non-essential, but beneficial trace nutrients can be most variable. Fe bioavailability is low both in aquatic and cropland environments, mainly because of its low solubility in the more oxidized, but most prevalent, Fe(III) state.^{172,173} Its central role in the abundant photosynthetic apparatus, which most primary producers depend on for carbon fixation, assures that Fe availability limits virtually all forms of life.^{174,175} An evolutionary adaptation in some photosynthetic organisms to low Fe environments was therefore to use a Cu-containing protein, plastocyanin, instead of the Fe-containing Cyt *c₆*, for the same function, namely, the transport of electrons between Cyt *b₆f* and photosystem 1.^{169,176} While this reduces the organisms' Fe quota, simultaneously, its dependence on Cu becomes greater. Other acclimation mechanisms also involve the intracellular recycling of metal cofactors and subsequent redistribution to other processes, according to a hierarchy of essentiality in the organism.^{177–180}

Intracellular over-accumulation of various elements beyond the necessary quota can also affect cell health and occurs either in polluted or otherwise nutrient-imbalanced environments. Plants, e.g. accumulate P when Zn is limiting and vice versa,^{181–183} while the green alga *Chlamydomonas* accumulates large amounts of Cu in Zn-limiting conditions.^{184,185} Sequestration in specialized, intracellular compartments is a common strategy to either detoxify over-accumulating, biologically undesired elements, store scarce nutrients in preparation for periods of limitation or for future generations, sequester a resource away from competitors, or buffer nutrients temporarily during metabolic transitions.^{186–189} Acidocalcisomes are lysosome-related organelles, first identified in trypanosomes but widely present in eukaryotes.¹⁹⁰ Acidocalcisomes are rich in Ca and P,^{191,192} in some organisms also K,¹⁹³ and can temporarily accumulate various micronutrient metals and toxic elements. The eukaryotic green alga *Chlamydomonas*, e.g. has been found to sequester the trace nutrients Cu, Mn, and Fe and the heavy metal Cd in acidocalcisomes in periods of over-accumulation.^{184,194–197}

Vacuoles in general are the most important storage sites in eukaryotes, including photosynthetic organisms,^{187,189,198} but other means of storage and sequestration can also be utilized. Proteins like ferritin, a soluble 24-subunit oligomer, can sequester trace elements, ~4500 Fe ions in ferritins case,^{199,200} and other organelles like the starch-separated pyrenoid in the chloroplast have been found to contribute to Cd sequestration.^{196,197,201}

Research of metal homeostasis not only aims to identify acclimation processes in natural settings but can also be exploited in bioremediation or biofortification applications. While heavy metals, $z > 20$, density $> 5 \text{ g/cm}^3$,²⁰² can be naturally present in specific soil or aquatic environments, more importantly, human activities, from mining and industrial production processes to domestic and agricultural practices, have led to an increased contamination of natural habitats with toxic metals.^{203–205} Cd, As, Pb, Cr, and Hg are thereby the most prominent elements, all presenting severe dangers to human health.²⁰³ While conventional methods like chemical precipitation, reverse osmosis, adsorption, or electrodeposition are used to remove heavy metals from environments, the use of biological organisms can be much more efficient and cost-effective.^{206,207} Photosynthetic algae, e.g. are uniquely positioned to be utilized in the removal of heavy metals in soil and aquatic environments, and research into their trace metal metabolism can greatly facilitate the effectiveness of these processes.^{208–210} Biofortification on the other hand, is a biotechnological process intended to increase the nutritional value of human nutrition, with major crop plants being generally poor sources of micronutrients.²¹¹ Targeting photosynthetic organisms like crops or algae, which are used as animal feed stocks or in natural supplements, is an efficient way to improve nutritional deficiencies.²¹²

Quantitative, intracellular elemental distributions

Whether it is for research or in the pursuit of biotechnological applications, the acquisition of spatially resolved, quantitative elemental maps is a key tool for researchers to identify the molecular mechanisms involved in elemental homeostasis. Elemental distribution can identify the function, specificity, and directionality of membrane transporters, which are involved in the uptake, removal, or intracellular distribution of specific nutrients in the cell. Transport mechanisms are equally involved in storage or sequestration efforts. Other proteins involved in elemental homeostasis, e.g. transcriptional/translational control factors, signal transduction components, chaperones, buffering/protective proteins or metabolites, and major client proteins, e.g. abundant enzymes requiring a specific elemental cofactor, are also required to achieve native elemental distribution. Using specific mutants and analyzing differential elemental distribution maps can facilitate the identification of the function of these proteins in the first place.²¹³ Detailed elemental distribution maps in different stages of nutrition for individual elements or upon other environmental perturbations (pH, temperature, light) can help in identifying the molecular mechanisms utilized in acclimation.

Therefore, over the past decades, a number of analytical techniques have been developed to determine intracellular elemental distribution, utilizing different properties to distinguish the elements. The various techniques all have different advantages and disadvantages, making the different applications quite complementary, especially with regards to sensitivity (detection limit and quantifiable range), obtainable spatial resolution, range of elements that can be (simultaneously) recorded, sample prepara-

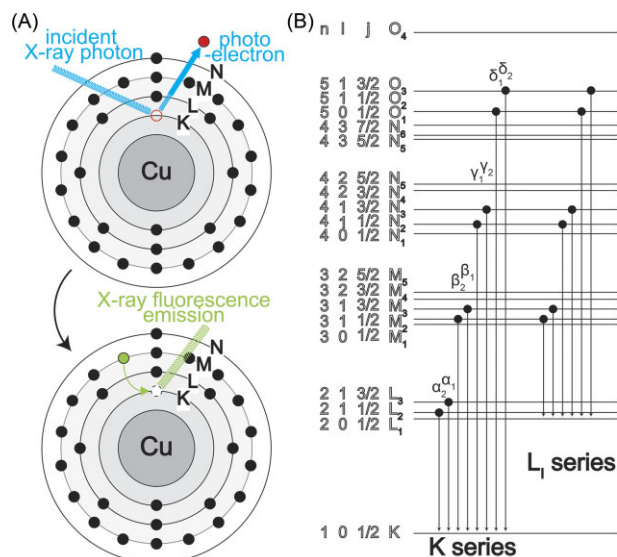


Fig. 2 Principle of X-ray fluorescence emission. (A) Exemplary schematic of the physics at a Cu atom. An incident X-ray photon from a synchrotron source with sufficient energy to excite a core electron, leaving a hole in the process, which is subsequently filled by an electron from a different shell while emitting fluorescence equivalent to the energy difference. (B) Overview of the nomenclature of different electron transitions. For X-ray fluorescence microscopy, the K and L series are the most relevant for detection.

tion, preservation, the amount of material required, and the kind of artefacts produced either from sample preparation or from the methodology itself. For detailed reviews of the individual methodologies see,^{214–216} and an in-depth discussion of strengths and weaknesses between the most common individual techniques can be found here.²¹⁷ Two major categories can be distinguished: (i) fluorescence microscopy-based techniques using element-sensitive dyes or genetically encoded metal-binding sensors and (ii) scanning technologies using either mass spectrometry [Laser Ablation Inductively Coupled Plasma Mass Spectrometry (LA-ICP-MS); nanoscale Secondary Ion Mass Spectrometry (nanoSIMS)] or the detection of element-specific energy signatures [Synchrotron Radiation X-Ray Fluorescence Microscopy, abbreviated either (XFM, XRF, SXRF, or SRXRF); Particle Induced X-ray Emission (PIXE); Energy Dispersive X-ray Spectroscopy, abbreviated either (EDX, EDS, or EDXS)] to determine the elemental composition.²¹⁴

The fluorescence microscopy-based techniques rely on the chemical properties of the individual molecular probe to identify a specific element, sometimes even a specific oxidation state, resulting in a fluorescence change (reversible or irreversible). Coupled with an adequate fluorescence microscope with the necessary resolution, which is available in many laboratories, the probes allow one to quickly analyze intracellular elemental distributions in many cells.²¹⁸ The analysis is limited to a set of compatible, non-overlapping fluorescent signals at a time, but the probes can be utilized in living cells to specifically assess the labile, accessible fraction of the element in the cell. Quantitation of the labile metal pool using fluorescence-based probes is possible,²¹⁹ but access to particularly tightly bound, or less accessible, sequestered elemental cofactors might preclude capturing the total metal distribution using probes.

Outside of the probe-based techniques, XFM is a popular choice to determine quantitative intracellular elemental maps.^{215,220} XFM takes advantage of the unique electron orbital configurations of each element (Fig. 2). Using a highly focused X-ray beam at an

energy above the binding energy of a core electron of an element can result in the removal of the electron from the atom. Upon removal, another electron from an outer shell can rapidly transition to the inner shell and fill the hole. The energy difference between the orbitals, specific for each transition (Fig. 2B), can be emitted as X-ray fluorescence, which can be recorded and analyzed using an energy-dispersive detector.²²¹ Using a highly focused incident X-ray beam and a precisely controllable sample stage, 2D-projection images of the elemental composition of the material in the path of the beam are then assembled spot by spot at high resolution. At this point, most research utilizes highly brilliant synchrotron radiation sources to fast determine subcellular distribution maps at nanoscale, crucially limiting the amount of cells that can be analyzed.²¹⁶ Benchtop systems, however, continue to improve in resolution²²² and can present an attractive route to improve access to elemental imaging in the future. There are >50 synchrotrons globally, many of them offering XFM capabilities; pixel sizes below 100 nm can be achieved at multiple beamlines at synchrotrons including,^{217,223–231} which is well below the threshold of what is generally considered subcellular resolution (<1 μm , nanometer scale). Due to the ability of X-ray photons to penetrate biological material, XFM can be used to examine much thicker samples compared to those used for electron microscopy, often removing the requirement for sectioning, especially for single-cell organisms, and therefore facilitating sample processing and whole-cell analysis simultaneously.

Mass spectrometry-based techniques (LA-ICP-MS or nanoscale SIMS) are alternative options, offering isotope-specific detection of elements.²³² In principle, these techniques use a highly focused laser (LA-ICP-MS) or ion beam (SIMS) to release material from a specific spot of a sample (cell section in the case of intracellular studies), which is then analyzed in a mass spectrometer for its elemental composition. Cs^+ and O^- ion beams have a high ionization potential, allowing the determination of intracellular elemental maps with high detail, even of elements present in trace amounts.^{184,215,232,233} This has several advantages over XFM. By using the mass of an element instead of the electron configuration for detection, individual isotopes of element can be distinguished, allowing time-course studies with specific isotopes in pulse-chase mode. Lower resolution images of regions of the sectioned material allow to analyze a larger number of cells than can be analyzed with XFM. Both MS-based applications are considered destructive, in the sense that material of the specimen is used for the analysis, compared to the techniques that probe electron configurations or molecular probes, which are generally considered non-destructive, not consuming material for the identification of an element. The radiation, however, used for both of these techniques can, nevertheless, induce changes in the sample during detection. Radiation damage to cell structures, especially with long dwell times or after repeated scans, is a concern.²³⁴ While submicron resolution has recently been achieved (0.6 μm spot size²³⁵), the resolution of LA-ICP-MS is still one order of magnitude lower than the other techniques, limiting its utility to determine high-resolution intracellular structures in eukaryotic alga. SIMS at nanoscale can achieve similar resolutions to XFM, sub-100 nm pixel size, but matrix effects have long been a challenge for quantitative aspects. Additionally, the inherent nature of mass-spectrometry applications, which rely on the removal of material for elemental analysis, makes it difficult, but not impossible, to analyze whole cells quantitatively, requiring subsequent, repeated scans of the same area to fully capture the three-dimensional cell.²³⁶

Eukaryotic algae as subjects

Eukaryotic algae are excellent subjects for quantitative elemental imaging studies. Algae is a term of convenience, combining several diverse eukaryotic groups of photosynthetic organisms.²³⁷ Many algae are unicellular eukaryotes of a size that is convenient for imaging applications; not too small to require too high of a resolution on the instrumentation end to determine subcellular distribution, but small enough to not require sectioning in applications that do not require it. They are important primary producers with crucial environmental roles, often inhabiting nutrient-limited environments on land or in the oceans, making them interesting research subjects. Green algae are within the Viridiplantae, which also contain the land plants. Together with the red algae (rhodophytes) and glaucophytes in the plantae supergroup, these algae are the result of primary endosymbiosis, where their chloroplasts arose from a free-living cyanobacterium.²³⁸ Outside the plant lineage, several diverse groups of algae are found: heterokonts (diatoms, brown algae), dinoflagellates, apicomplexans, haptophytes, cryptomonads, euglenoids, and chlorarachniophytes are all eukaryotic algae resulting from secondary or tertiary endosymbiosis, receiving their chloroplast from a eukaryotic donor.^{237,239} Within these groups, several organisms have been analyzed in detail, but probably no individual alga more than the green alga *Chlamydomonas reinhardtii*, and no group more than the diatoms of the genus *Thalassiosira*.

Chlamydomonas reinhardtii is a unicellular green alga that has been widely used as a eukaryotic, photosynthetic reference system. It is a haploid, facultative phototroph with a short generation time (~6 h in the presence of a reduced carbon source). Its genome has been fully sequenced, and all three genomes can be targeted for modification.^{240,241} *Chlamydomonas* has been widely used for research on algal metabolism, and has served as a resource for commercial applications of algae as sources of biofuels or bioproducts.^{242, 243} Its common ancestry with land plants, albeit distant (>1 billion years ago), allows for cross-comparisons to the intensively studied plant systems, and research performed in either to be cross-informative. Yet *Chlamydomonas* is less complex (single, uniform cell), contains smaller gene families and less complex gene structures. In terms of elemental composition, the photosynthetic electron transfer chain is virtually identical with that in land plants, and the alga utilizes a broad spectrum of metal cofactors to sustain its photosynthetic, respiratory, and metabolic capabilities. In the past decades, studies have been carried out to identify the major transporters involved in nutrient acquisition and distribution.^{156,185,244–248} Mechanisms for nutrient-sparing and recycling have been discovered,^{169,177,249–251} and storage sites were identified,^{156,184,194,195,252–254} making this organism particularly useful for elemental analysis studies.

Thalassiosira is a genus of centric diatoms found in diverse marine and freshwater ecosystems, widely recognized for their substantial contribution to global primary productivity.^{255–257} Their defining feature is the silicified cell walls, consisting of species-specific, fine-scaled nano-structures that are built intracellularly in a specialized compartment before being exported to assemble the cell wall.²⁵⁸ The genus contains mostly single-celled species, but, especially in marine species, the single cells can be connected via chitin fibrils to 'string of beads' colonies.²⁵⁷ The genomes of *Thalassiosira pseudonana*²⁵⁹ and *Thalassiosira oceanica*²⁶⁰ have been fully sequenced, and protocols for genetic manipulation of *T. pseudonana*²⁶¹ and *Thalassiosira weissflogii*²⁶² have been developed. *Thalassiosira*'s elemental metabolism has been of particular interest to researchers, especially that of silicon, with regards to

the synthesis of its cell wall, and iron, with regards to iron's role in limiting the growth of alga in oceanic, high nutrient/low chlorophyll environments, restricting their potential for carbon sequestration.^{260,263–266} Algae have been excellent subjects for elemental imaging studies from the beginning; early work developing XFM instrumentation already involved images of diatoms.²⁶⁷ The first elemental distribution maps of eukaryotic algae using fully developed XFM setups were also taken from diatoms, *T. weissflogii*, and natural isolates with 0.5 μm step size at the Advanced Photon Source (APS, Argonne, USA).^{268,269} The authors established the quantitative capabilities for Si, Mn, Fe, Ni, and Zn in single cell analysis and determined the detection limits of the technique. The setup was later used by Twining *et al.* to determine the Fe distribution in natural diatom and dinoflagellate isolates upon ocean iron fertilization,²⁷⁰ or in specific oceanic regions.²⁷¹ Adams *et al.* used it to determine Cu distribution in the diatoms *Phaeodactylum tricorutum* and *Ceratoneis closterium*, as well as in the green alga *Tetraselmis* sp.²⁷² Nuester *et al.* determined the Fe distribution in a similar setup with improved resolution, 0.2 μm step size, in the diatoms *T. pseudonana* and *T. weissflogii*.²⁷³ Another diatom, *Cyclotella meneghiniana*, was used in a study by de Jonge *et al.*, significantly improving the resolution of XFM tomography to a useful range (<400 nm) for single cells smaller than 10 μm diameter.²⁷⁴ Diaz *et al.* demonstrated the utility of XFM for green alga research, using *Chlamydomonas* and *Chlorella* species to demonstrate Fe sequestration in stationary cells.²⁷⁵ Elemental maps of Fe, Zn, and K were obtained from frozen hydrated *Chlamydomonas* cells with <100 nm spatial resolution during the development of the Bionanoprobe at the Advanced Photon Source.²²³ The alga, together with a different green alga, *Ostreococcus* sp., was also the subject for demonstrating the utility of ptychography, a coherent diffraction imaging technique that uses multiple overlapping regions of a cell to provide superior spatial resolution. Deng *et al.* demonstrated <20 nm spatial resolution of ultrastructure imaging of frozen-hydrated algae with ptychography while simultaneously recording fluorescence spectra to determine the intracellular P, Ca, K, and S distributions.^{193,276} 3D reconstruction of cellular P, Ca, S, Cl, and K distributions and ultrastructure from ptychographic tomography using GENFIRE also took advantage of *Chlamydomonas*.²⁷⁷ Outside of method development, XFM has proven useful for the characterization of intracellular metal sequestration sites in *Chlamydomonas* at the APS, and at the European Synchrotron Radiation Facility (ESRF, Grenoble, France). Researchers found Fe, Cu, and Mn to be sequestered in cytosolic vacuoles, acidocalcisomes,^{184,194,195} while the heavy metal Cd was found to be localized both in acidocalcisomes and the pyrenoid in the chloroplast.^{196,201} Similarly, the green alga *Coccomyxa actinabiotis* was analyzed at 100 nm resolution in studies aimed at identifying the mechanisms for Co and Ag tolerance.²⁷⁸ Coccolithophores, eukaryotic algae from the haptophytes and renowned for their calcite exoskeleton, were analyzed for elemental distributions up to Sr using XFM at 50 nm resolution in artificial seawater enriched with trace nutrients.²⁷⁹ They were also the subject of an X-ray ptychography tomography study at 30 nm resolution determining their ultrastructure.²⁸⁰

Controlling variance in elemental composition of algae

Successful elemental imaging for elemental imaging starts with a controlled elemental environment during cultivation of the alga. For this reason, a chemically defined medium is superior to a complex medium recipe. For *Chlamydomonas*, the most popu-

lar media are TAP/TP and HS/HSM (\pm acetate as a reduced carbon source), which are both chemically defined.²⁸¹ Avoiding components like sea water, peptone, or yeast extract would be ideal if possible. Both *Chlamydomonas* media originally used a trace element mixture recipe developed by Hutner,²⁸² which can vary substantially in its content in between batches. Hutner's solution was not specifically optimized for the alga; specifically, it lacks Se completely but contains both Co and B, which are not utilized by the alga.²⁸³ Instead of the single trace element additive derived from Hutner, a 7-solution trace element suite was developed specifically for *C. reinhardtii*, which changed the composition accordingly and additionally adjusted the concentrations of the other trace elements (especially Zn but also Fe, Cu, and Mn) to better match the algae's metabolic demand.²⁸³ The use of controlled, high-purity chemicals for media preparation additionally ensures reproducible conditions. The water, glass, and plasticware used for media preparation and cultivation should be low in contaminants. Acid-washing of glassware is recommended, overnight incubation in 6N HCl followed by thorough rinsing in clean water to remove residual HCl.²⁸⁴ Depending on the condition of interest, liquid pre-cultures used for inoculation at a specific cell density, already grown in the elemental condition intended for analysis, additionally improve the reproducibility between experiments, which can be useful if there are long periods in between replicates (e.g. in between beamline visits).

Sample preparation for XFM measurements

The most crucial component of sample preparation is the trade-off between the necessity to deliver the sample material in the required form to the imaging application of choice and to simultaneously preserve the sample material in an unaltered state that reflects the condition that is analyzed.²¹⁷ Long incubation steps, changes in temperature, necessary concentration steps (centrifugation), or buffer changes to accommodate fixation can potentially alter the state of the sample material on its way from its habitat (or the growth chamber in a laboratory) to the imaging application. For photosynthetic organisms, changes in illumination and aeration during sample preparation are also potentially critical, as they can affect metabolism quickly.^{285,286} Metal-sensitive probes compatible with live cell imaging are probably the gold standard in this regard, allowing the researcher to keep cells as close to the state of interest as possible. For XFM, rapid vitrification of cells in liquid ethane (e.g. using a FEI Vitrobot Mark IV plunge freezer^{193,223,276,277} or similar) is minimally invasive, and preserves the cell in a frozen hydrated state. Successful settings for vitrification of *Chlamydomonas* on the Vitrobot were reported at a temperature between 20 and 22°C, humidity of 100%, with a blot time of 2 s at blot force 0, blot total 1,^{193,276,277} or a blot time of 3 s at blot force 2, blot total 1, wait and drain time of 0 s.¹⁹⁵ For this to be effective, the beamline needs to support imaging at low temperatures,^{223,226} and the samples to never thaw after the initial freezing event. A major limitation to using vitrification for sample preparation is the availability of cryo-XFM instruments capable of performing subcellular analyses at low temperatures, and access to specific equipment like plunge freezers can also be prohibitive. Additionally, cryo-preserved samples can collect ice deposits from environmental humidity, especially during, even very brief, transfers between any type of equipment (plungers, microscopes, XFM instruments, and storage/shipping vessels), which can result in a loss of the ability to produce a useful XFM image from the sample. Alternatively, chemical fixation (e.g. using 4% paraformaldehyde)

at an early stage of sample preparation is still used and effective, and allows imaging to take place at XFM instruments at room temperature. The elements of interest are crucial in the choice of fixation for any specific study. Chemical fixation, especially using various popular aldehydes, can be problematic for the preservation of the native state, especially of highly diffusible ions, e.g. Na, K, and Cl.^{226,287} A previous study¹⁹⁵ showed that the intracellular amounts of Fe and Cu were similar in vitrified and chemically fixed cells, and the distribution patterns were comparable with chemical fixation, albeit not as crisp as in the frozen-hydrated cells. Aldehydes can also alter membrane permeability,²⁸⁷ which might affect intracellular distribution.

In both cases, the cell material needs to be transferred either to film¹⁹⁶ or Si₃N₄ windows,^{193–195,223,276,277} compatible with the downstream beamlines, prior to freeze-plunging or chemical fixation. More elaborate analyses like ptychography or tomography reconstruction might require specific sample holders or additional sample preparation, which should ideally already be considered at this stage. The Si₃N₄ windows can be pretreated with poly-L-lysine to improve adhesion of alga cells (a single droplet of poly-L-lysine applied to the window and incubated for 30 min at 37 °C before the remainder of the droplet is removed and the cells are spotted). For quantitative applications, the cells need to be freed from media remnants,^{195,196} with brief washing steps (ideally with water as the last step), which has to be done prior to freeze plunging,²⁷⁸ but can be done after chemical fixation, when cells are already spotted on the carrier.¹⁹⁵ Washing is crucial, but extended washing can reduce the number of cells on the sample holder. The force by which the washing solution is applied to and removed from the sample holder contributes to the displacement. Using poly-L-lysine to assist in adhesion, a good starting point for the cell concentration of a motile *Chlamydomonas* culture to be spotted on a Si₃N₄ window was found to be 1×10^7 cells/ml, spotting between 50 and 100 μ l.¹⁹⁵ The concentration of the cells on the sample holder is crucial and should be optimized with the sample preparation procedure in place at a light microscope beforehand. If too many cells are spotted, then the analysis becomes significantly more complex, as X-rays can penetrate multiple layers of cells, and the resulting fluorescence will be reflective of all cellular material in the path of the beam. The identification of individual cells at the beamline becomes also more tedious, curiously, too little cells on the holder will do the same, by increasing the time of search and movements in between the positions of individual cells; a healthy balance is therefore ideal. In addition, the emitted fluorescent X-rays used to identify elemental speciation at each spot penetrate biological material less efficiently as the incident X-ray beam, which might result in a loss of fluorescent signal in thicker samples, affecting either the accuracy of the quantitation or even the correct identification of the elemental content at each spot. Controls, like a comparative quantitative analysis of bulk material in parallel to the imaging analysis, allow one to identify problems of this kind during method development.^{195,288}

Determining elemental distribution maps with XFM

Measurement at the individual beamlines will be dominated by the requirements and specifications of the respective instruments. Samples should be in a state, either by fixation or freezing, to withstand the loading and analysis procedures. Calibration of the X-ray fluorescence emission data is required to allow absolute quantitation of the spatially distributed data. The principle and

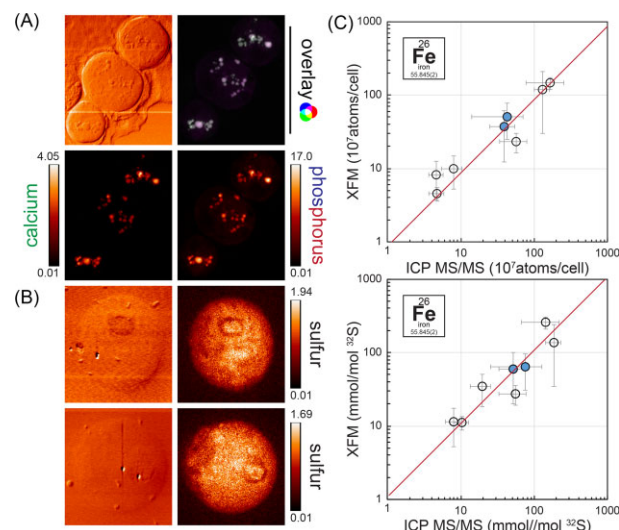


Fig. 3 Element distribution identifying organelles and spatial normalization using S. (A) Phosphorus and calcium distribution in *Chlamydomonas* cells, as well as the overlay, showing acidocalcisomes in Zn deficiency. (B) Sulfur distribution in *Chlamydomonas* cells, potentially showing starch sheets and pyrenoids. (C) Correlation of Fe content as measured by X-ray fluorescence microscopy (x-axis) and ICP-MS/MS (y-axis), normalized either per cell (top) or using S content (bottom), also determined either with ICP-MS or via XFM. Error bars in x and y directions indicate standard deviation in the measurements between at least four individual cells (XFM) or between at least between three independent cultures (ICP-MS/MS). Blue fill indicates frozen hydrated samples; gray fill indicates chemical fixation.

different strategies are nicely summarized in this review.²⁸⁹ Briefly, calibration is usually done by comparing the intensity of the fluorescence signal emitted from the individual samples to a calibration curve developed from the measurement of standard thin films containing a few elements with known concentrations.²⁹⁰ Matrix matching of the standards and samples is very difficult,²⁸⁹ standards used can therefore be quite different in nature from the biological material analyzed. An in-parallel analysis of the elemental composition of the bulk sample material provided for the spatial analysis by other means, e.g. ICP-MS, is therefore of advantage and can be used at later stages to interrogate the spatial quantitation of the material.^{195,278} Additionally, single-cell organisms like *Chlamydomonas* grown in asynchronous conditions in constant light (the most typical way) will contain a mixture of cells at various stages in the cell cycle.^{291–294} The elemental composition of cells can vary with the growth stage of the cells, and specific observations with respect to the elemental composition might be tied to an individual stage of the cell cycle. Synchrotron beamline time allocation is a crucial limiting factor, especially for quantitative experiments, with respect to the number of cells that can be analyzed at the required spatial resolution. Nevertheless, similar to other microscopy techniques, a mixture of cells from different developmental stages should be selected, as much as possible, to reduce the risk of conclusions based on a biased subset. The size of a cell can inform ‘on which developmental stage’ an individual cell in a batch culture from an asynchronous population currently resides; therefore, selecting cells of various sizes is a straightforward way to avoid oversampling of a specific condition. This can either be done prior to beamline visits, using a light microscope and some coordinate system to record the cell position, or at the beamline. Scans at a lower resolution prior to data collection are routinely used to minimize instrument time by optimizing the focus area of the cell of interest. They also allow

for a first assessment of cell size and ensure cell integrity prior to analysis. This selection process, while crucial, can later contribute to the variance in the quantitative data, especially when the data are normalized per cell.

Data analysis of spatially distributed elemental data

Analysis of the acquired emission spectra can be divided into two parts: an accurate quantitation of the data coming from the instrument and a subsequent analysis of the data in between different cells and conditions using normalization and statistics. In the first part, different options and strategies are discussed in detail in an excellent review.²²¹ In brief, quantification of fluorescence data can already be achieved by simple binning of counts within a certain energy window. While this can be sufficiently accurate, peak-fitting to determine the area in the same energy window, especially when combined with correcting for background levels or overlapping peaks, has been demonstrated to be more accurate and should be preferentially used if available. Software tools^{230,295–297} greatly facilitate all aspects of image analysis, including fitting, ROI analyses, and co-localizations. A detailed step-by-step protocol on how to perform and evaluate XFM data fitting using the MAPS software package can be found here.²⁹⁸

For the subsequent quantitative image analysis, software tools are also of great assistance because they allow the extraction of the quantified information for each pixel and can summarize it both for the whole image globally and for selected regions of interest. Initially, we recommend dividing the image into two regions: the part of the image that is covered by the cell and the surrounding region.^{195,278} This can be done either manually or algorithm assisted using an abundant element with good signal-to-noise contrast between the cell and the background, e.g. S. Both regions contain valuable information. The background, within the same image, contains the signal recovered from the sample holder and remnants of the sample preparation process, which should be subtracted from the biological material to obtain the total cellular content for each of the identified elements. XFM results are determined as the amount of element/area, summarizing the total amount of material in the column of the beam. For background correction, the amount/area in the background is subtracted from the amount/area in the area covered by the cell before the total cellular amount is calculated from the area covered by the cell. The amounts of elements in the background region should ideally be small compared to the cell image; if there is a substantial amount of elements of interest in the background, then additional washing steps should be added to the sample preparation procedure for the next batch; two consecutive washes of the already spotted cells on the sample holder with clean water were sufficient to have <1% of elements of interest/area in the background region compared to the region covered by the cell. The background-corrected cellular content obtained this way can directly be compared to alternative means of quantitation (e.g. ICP-MS). The quantitative data from this analysis can also be used to evaluate technical aspects, like different approaches to fixation (chemically fixed versus frozen hydrated samples from the same batch), in-between batch variation, or different sample preparation strategies.

Comparisons between different intracellular features are achieved by identifying individual organelles from differential phase contrast images or ptychography reconstruction, or by algorithm-assisted identification of specific elemental signatures within the cells. In *Chlamydomonas*, acidocalcisomes, cytosolic

vacuoles with a role in trace metal sequestration (Fig. 3A), are rich in P and Ca, and potentially also K.^{184,194,195,276,299} contractile vacuoles, involved in osmoregulation, are rich in K and Cl;^{254,300,301} pyrenoids, sites of concentrated CO₂ fixation in the chloroplast, might have slightly increased S content;¹⁹⁶ and large starch shields surrounding the pyrenoid might be visible by the absence of individual elements (Fig. 3B). Other organelles or cellular structures can have a distinguishable elemental composition only in specific nutritional or developmental stages or upon genetic changes, which might then also present an opportunity for selection and further analysis. When algorithm-assisted means are used, it is important to ensure that all the identified regions are completely contained within the cell of interest. Remnants from cell lysis or other cells within the same imaging window might complicate the issue. When intracellular regions are compared, additional normalization or statistical evaluations are necessary to account especially for variance in thickness of the material in the way of the beam. Areas in the center of single cells, where thickness is high compared to peripheral regions, will naturally have a higher amount of element in the 2D projection. Several methods to determine thickness experimentally are discussed previously;²²¹ a more direct way to deal with bias is to utilize a strength of XFM and identify a different elemental distribution from the same cell that shows a uniform distribution, e.g. S (Fig. 3C), and use that for normalization of enrichment analysis.¹⁹⁵

Conclusion

Eukaryotic algae are crucial primary producers in soil, oceanic, and freshwater environments. Their habitats suffer from low trace nutrient bioavailability or heavy metal pollution, sparking research interest into the mechanisms of their metal metabolism. The strategies involved in trace metal distribution can be exploited for biotechnological utilization, either to improve algae growth and consequently their potential for carbon sequestration, for biofortification, or to utilize their mitigation strategies in bioremediation applications. XFM can be a powerful tool to investigate the intracellular elemental distribution of (trace) nutrients in eukaryotic algae quantitatively, allowing to assign function to individual components involved in managing elemental homeostasis or identifying acclimation strategies or useful phenotypes. This Tutorial Review summarizes the state of research involving sub-cellular elemental distributions determined using XFM with eukaryotic algae as subjects, and provides a workflow of a quantitative elemental distribution analysis for eukaryotic alga.

Funding

S.S. and S.S.M. are supported by a grant from the U.S. Department of Energy, Office of Science, Basic Energy Sciences (DE-SC0020627) for their work on iron metabolism. S.S.M. work on Cu is supported by a grant from the National Institutes of Health (GM42143). S.C.'s effort is partially supported by a grant from the U.S. Department of Energy (PRJ1009594) and the U.S. Department of Energy, Argonne National Laboratory (DE-AC02-06CH11357).

Conflict of interest

The authors declare no conflicts of interest.

Data availability

The data underlying this review are available in the article and in its online supplementary material.

References

1. D. I. Arnon and P. R. Stout, The essentiality of certain elements in minute quantity for plants with special reference to copper, *Plant Physiol.*, 1939, 14(2), 371–375. <https://doi.org/10.1104/pp.14.2.371>
2. T. F. N. Ramblings, “Chnops,” plus, *Sci. News Lett.*, 1936, 30(801), 110. <https://doi.org/10.2307/3912915>
3. S. J. Lippard and J. M. Berg, *Principles of Bioinorganic Chemistry*. University Science Books, Mill Valley, 1994.
4. S. S. Merchant and J. D. Helmann, Elemental economy: microbial strategies for optimizing growth in the face of nutrient limitation, *Adv. Microb. Physiol.*, 2012, 60, 91–210. <https://doi.org/10.1016/B978-0-12-398264-3.00002-4>
5. C. Andreini, I. Bertini, G. Cavallaro, G. L. Holliday and J. M. Thornton, Metal ions in biological catalysis: from enzyme databases to general principles, *J. Biol. Inorg. Chem.*, 2008, 13(8), 1205–1218. <https://doi.org/10.1007/s00775-008-0404-5>
6. K. J. Waldron, J. C. Rutherford, D. Ford and N. J. Robinson, Metalloproteins and metal sensing, *Nature*, 2009, 460(7257), 823–830. <https://doi.org/10.1038/nature08300>
7. Y. Wang and W. H. Wu, Potassium transport and signaling in higher plants, *Annu. Rev. Plant Biol.*, 2013, 64(1), 451–476. <https://doi.org/10.1146/annurev-arplant-050312-120153>
8. R. A. Leigh and R. G. W. Jones, A hypothesis relating critical potassium concentrations for growth to the distribution and functions of this ion in the plant-cell, *New Phytol.*, 1984, 97(1), 1–13. <https://doi.org/10.1111/j.1469-8137.1984.tb04103.x>
9. J. Cui and G. Tcherkez, Potassium dependency of enzymes in plant primary metabolism, *Plant Physiol. Biochem.: PPB*, 2021, 166(September), 522–530. <https://doi.org/10.1016/j.plaphy.2021.06.017>
10. R. M. Wynn, R. Ho, J. L. Chuang and D. T. Chuang, Roles of active site and novel K⁺ ion-binding site residues in human mitochondrial branched-chain alpha-ketoacid decarboxylase/dehydrogenase, *J. Biol. Chem.*, 2001, 276(6), 4168–4174. <https://doi.org/10.1074/jbc.M008038200>
11. M. Hauer-Jakli and M. Trankner, Critical leaf magnesium thresholds and the impact of magnesium on plant growth and photo-oxidative defense: a systematic review and meta-analysis from 70 years of research, *Front. Plant Sci.*, 2019, 10, 766. <https://doi.org/10.3389/fpls.2019.00766>
12. Z. C. Chen, W. T. Peng, J. Li and H. Liao, Functional dissection and transport mechanism of magnesium in plants, *Semin. Cell Dev. Biol.*, 2018, 74(February), 142–152. <https://doi.org/10.1016/j.semdb.2017.08.005>
13. D. J. Klein, P. B. Moore and T. A. Steitz, The contribution of metal ions to the structural stability of the large ribosomal subunit, *RNA*, 2004, 10(9), 1366–1379. <https://doi.org/10.1261/rna.7390804>
14. R. Willstätter, Zur kenntniss der zusammensetzung des chlorophylls, *Justus Liebigs Ann. Chem.*, 1906, 350(1-2), 48–82. <https://doi.org/https://doi.org/10.1002/jlac.19063500103>
15. A. C. Storer and A. Cornish-Bowden, Concentration of MgATP²⁻ and other ions in solution. Calculation of the true concentrations of species present in mixtures of associating ions, *Biochem. J.*, 1976, 159(1), 1–5. <https://doi.org/10.1042/bj1590001>
16. G. L. Wheeler and C. Brownlee, Ca²⁺ signalling in plants and green algae—changing channels, *Trends Plant Sci.*, 2008, 13(9), 506–514. <https://doi.org/10.1016/j.tplants.2008.06.004>
17. Y. Umena, K. Kawakami, J.-R. Shen and N. Kamiya, Crystal structure of oxygen-evolving photosystem II at a resolution of 1.9 Å, *Nature*, 2011, 473(7345), 55–60. <https://doi.org/10.1038/nature09913>
18. A. Weber, On the role of calcium in the activity of adenosine 5'-triphosphate hydrolysis by actomyosin, *J. Biol. Chem.*, 1959, 234(10), 2764–2769. [https://doi.org/https://doi.org/10.1016/S0021-9258\(18\)69777-7](https://doi.org/https://doi.org/10.1016/S0021-9258(18)69777-7)
19. R. Chattopadhyaya, W. E. Meador, A. R. Means and F. A. Quijcho, Calmodulin structure refined at 1.7 Å resolution, *J. Mol. Biol.*, 1992, 228(4), 1177–1192. [https://doi.org/10.1016/0022-2836\(92\)90324-D](https://doi.org/10.1016/0022-2836(92)90324-D)
20. M. J. Lenaeus, T. M. Gamal El-Din, C. Ing, K. Ramanadane, R. Pomes, N. Zheng and W. A. Catterall, Structures of closed and open states of a voltage-gated sodium channel, *Proc. Natl. Acad. Sci. USA*, 2017, 114(15), E3051–E3E60. <https://doi.org/10.1073/pnas.1700761114>
21. M. T. Lai, E. Di Cera and J. A. Shafer, Kinetic pathway for the slow to fast transition of thrombin. Evidence of linked ligand binding at structurally distinct domains, *J. Biol. Chem.*, 1997, 272(48), 30275–30282. <https://doi.org/10.1074/jbc.272.48.30275>
22. A. Peracchi, A. Mozzarelli and G. L. Rossi, Monovalent cations affect dynamic and functional properties of the tryptophan synthase alpha 2 beta 2 complex, *Biochemistry*, 1995, 34(29), 9459–9465. <https://doi.org/10.1021/bi00029a022>
23. T. Murata, I. Yamato, Y. Kakinuma, A. G. Leslie and J. E. Walker, Structure of the rotor of the V-Type Na⁺-ATPase from *Enterococcus hirae*, *Science*, 2005, 308(5722), 654–659. <https://doi.org/10.1126/science.1110064>
24. F. Brini and K. Masmoudi, Ion transporters and abiotic stress tolerance in plants, *ISRN Mol. Biol.*, 2012, 2012, 927436. <https://doi.org/10.5402/2012/927436>
25. T. Stauber, S. Weinert and T. J. Jentsch, Cell Biology and physiology of CLC chloride channels and transporters, *Compr. Physiol.*, 2012, 2(3), 1701–1744
26. G. Feller, T. Lonhienne, C. Deroanne, C. Libiouille, J. Van Beeumen and C. Gerday, Purification, characterization, and nucleotide sequence of the thermolabile alpha-amylase from the antarctic psychrotroph *Alteromonas haloplanctis* A23, *J. Biol. Chem.*, 1992, 267(8), 5217–5221. [https://doi.org/10.1016/S0021-9258\(18\)42754-8](https://doi.org/10.1016/S0021-9258(18)42754-8)
27. D. I. Arnon and F. Whatley, Is chloride a coenzyme of photosynthesis? *Science*, 1949, 110(2865), 554–556.
28. D. Oesterhelt, Structure and function of halorhodopsin, *Isr. J. Chem.*, 1995, 35(3-4), 475–494. <https://doi.org/10.1002/ijch.199500044>
29. D. E. Salt, I. Baxter and B. Lahner, Ionomics and the study of the plant ionome, *Annu. Rev. Plant Biol.*, 2008, 59(1), 709–733. <https://doi.org/10.1146/annurev-arplant.59.032607.092942>
30. M. J. Page and E. Di Cera, Role of Na⁺ and K⁺ in enzyme function, *Physiol. Rev.*, 2006, 86(4), 1049–1092. <https://doi.org/10.1152/physrev.00008.2006>
31. K. L. Britton, S. J. Langridge, P. J. Baker, K. Weeradechapon, S. E. Sedelnikova, J. R. De Lucas, D. W. Rice and G. Turner, The crystal structure and active site location of isocitrate lyase from the fungus *Aspergillus nidulans*, *Structure*, 2000, 8(4), 349–362. [https://doi.org/10.1016/S0969-2126\(00\)00117-9](https://doi.org/10.1016/S0969-2126(00)00117-9)
32. E. Giachetti, G. Pinzauti, R. Bonaccorsi and P. Vanni, Isocitrate lyase from *Pinus pinea*, *Eur. J. Biochem.*, 1988, 172(1), 85–91. <https://doi.org/10.1111/j.1432-1033.1988.tb13859.x>
33. V. K. Yachandra and J. Yano, Calcium in the oxygen-evolving complex: structural and mechanistic role determined by X-ray spectroscopy, *J. Photochem. Photobiol. B*, 2011, 104(1-2), 51–59. <https://doi.org/10.1016/j.jphotobiol.2011.02.019>
34. A. Mehri, Trace elements in human nutrition (II)—an update, *Int. J. Prev. Med.*, 2020, 11, 2. https://doi.org/10.4103/ijpvm.IJPVM_48_19

35. E. Andresen, E. Peiter and H. Kupper, Trace metal metabolism in plants, *J. Exp. Bot.*, 2018, 69(5), 909–954. <https://doi.org/10.1093/jxb/erx465>
36. J. Morrissey and C. Bowler, Iron utilization in marine cyanobacteria and eukaryotic algae, *Front. Microbiol.*, 2012, 3(43), 43. <https://doi.org/10.3389/fmicb.2012.00043>
37. L. R. Le Canu, J. L. Gay-Lussac and G. S. Sérullas. *De l'hématosine, ou matiere colorante du sang*. Mme. Huzard, 1830.
38. K. Tagawa and D. I. Arnon, Ferredoxins as electron carriers in photosynthesis and in the biological production and consumption of hydrogen gas, *Nature*, 1962, 195(4841), 537–543. <https://doi.org/10.1038/195537a0>
39. S. S. Merchant, S. Schmollinger, D. Strenkert, J. L. Moseley and C. E. Blaby-Haas, From economy to luxury: copper homeostasis in *Chlamydomonas* and other algae, *Biochim. Biophys Acta Mol. Cell Res.*, 2020, 1867(11), 118822. <https://doi.org/10.1016/j.bbamcr.2020.118822>
40. S. Katoh, A new copper protein from *Chlorella ellisoidea*, *Nature*, 1960, 186(4724), 533–534.
41. T. Tsukihara, H. Aoyama, E. Yamashita, T. Tomizaki, H. Yamaguchi, K. Shinzawa-Itoh, R. Nakashima, R. Yaono and S. Yoshikawa, Structures of metal sites of oxidized bovine heart cytochrome c oxidase at 2.8 Å, *Science*, 1995, 269(5227), 1069–1074. <https://doi.org/10.1126/science.7652554>
42. H. Beinert, D. E. Griffiths, D. C. Wharton and R. H. Sands, Properties of the copper associated with cytochrome oxidase as studied by paramagnetic resonance spectroscopy, *J. Biol. Chem.*, 1962, 237(7), 2337–2346. [https://doi.org/10.1016/S0021-9258\(19\)63443-5](https://doi.org/10.1016/S0021-9258(19)63443-5)
43. E. Stotz, C. J. Harrer and C. G. King, A study of “ascorbic acid oxidase” in relation to copper, *J. Biol. Chem.*, 1937, 119(2), 511–522. [https://doi.org/10.1016/S0021-9258\(18\)74396-2](https://doi.org/10.1016/S0021-9258(18)74396-2)
44. X. Hu, X. Wei, J. Ling and J. Chen, Cobalt: an essential micronutrient for plant growth?, *Front. Plant Sci.*, 2021, 12(2370), 768523. <https://doi.org/10.3389/fpls.2021.768523>
45. E. L. Smith, Presence of cobalt in the anti-pernicious anaemia factor, *Nature*, 1948, 162(4108), 144–145. <https://doi.org/10.1038/162144b0>
46. E. L. Rickes, N. G. Brink, F. R. Koniuszy, T. R. Wood and K. Folkers, Vitamin-B12, a cobalt complex, *Science*, 1948, 108(2797), 134. <https://doi.org/10.1126/science.108.2797.134>
47. D. C. Hodgkin, J. Kamper, M. Mackay, J. Pickworth, K. N. Trueblood and J. G. White, Structure of vitamin B12, *Nature*, 1956, 178(4524), 64–66. <https://doi.org/10.1038/178064a0>
48. C. C. Fabiano, T. Tezotto, J. L. Favarin, J. C. Polacco and P. Mazzafera, Essentiality of nickel in plants: a role in plant stresses, *Front. Plant Sci.* 2015, 6, 754. <https://doi.org/10.3389/fpls.2015.00754>
49. M. Alfano and C. Cavazza, Structure, function, and biosynthesis of nickel-dependent enzymes, *Protein Sci.*, 2020, 29(5), 1071–1089. <https://doi.org/10.1002/pro.3836>
50. N. E. Dixon, C. Gazzola, R. L. Blakeley and B. Zerner, Jack bean urease (EC 3.5.1.5). Metalloenzyme. Simple biological role for nickel, *J. Am. Chem. Soc.*, 1975, 97(14), 4131–4133. <https://doi.org/10.1021/ja00847a045>
51. A. Volbeda, M.-H. Charon, C. Piras, E. C. Hatchikian, M. Frey and J. C. Fontecilla-Camps, Crystal structure of the nickel-iron hydrogenase from *Desulfovibrio gigas*, *Nature*, 1995, 373(6515), 580–587. <https://doi.org/10.1038/373580a0>
52. S. Alejandro, S. Holler, B. Meier and E. Peiter, Manganese in plants: from acquisition to subcellular allocation, *Front. Plant Sci.*, 2020, 11, 300. <https://doi.org/10.3389/fpls.2020.00300>
53. A. Zouni, H.-T. Witt, J. Kern, P. Fromme, N. Krauss, W. Saenger and P. Orth, Crystal structure of photosystem II from *Synechococcus elongatus* at 3.8 Å resolution, *Nature*, 2001, 409(6821), 739–743. <https://doi.org/10.1038/35055589>
54. A. S. Mildvan, M. C. Scrutton and M. F. Utter, Pyruvate carboxylase: VII. A possible role for tightly bound manganese, *J. Biol. Chem.*, 1966, 241(15), 3488–3498. [https://doi.org/10.1016/S0021-9258\(18\)99859-5](https://doi.org/10.1016/S0021-9258(18)99859-5)
55. M. C. Scrutton, M. F. Utter and A. S. Mildvan, Pyruvate carboxylase: VI. The presence of tightly bound manganese, *J. Biol. Chem.*, 1966, 241(15), 3480–3487. [https://doi.org/10.1016/S0021-9258\(18\)99858-3](https://doi.org/10.1016/S0021-9258(18)99858-3)
56. K. A. McCall, C. Huang and C. A. Fierke, Function and mechanism of zinc metalloenzymes, *J. Nutr.*, 2000, 130(5S Suppl), 1437S–1446S. <https://doi.org/10.1093/jn/130.5.1437S>
57. D. Keilin and T. Mann, Carbonic anhydrase. Purification and nature of the enzyme, *Biochem. J.*, 1940, 34(8-9), 1163–1176. <https://doi.org/10.1042/bj0341163>
58. A. Liljas, K. K. Kannan, P. C. Bergstén, I. Waara, K. Fridborg, B. Strandberg, U. Carlbom, L. Järup, S. Lövgren and M. Petef, Crystal structure of human carbonic anhydrase C, *Nat. New Biol.*, 1972, 235(57), 131–137. <https://doi.org/10.1038/newbio235131a0>
59. M. Cassandri, A. Smirnov, F. Novelli, C. Pitolli, M. Agostini, M. Malewicz, G. Melino and G. Raschella, Zinc-finger proteins in health and disease, *Cell Death Discov.*, 2017, 3(1), 17071. <https://doi.org/10.1038/cddiscovery.2017.71>
60. J. S. Hanas, D. J. Hazuda, D. F. Bogenhagen, F. Y. Wu and C. W. Wu, Xenopus transcription factor A requires zinc for binding to the 5 S RNA gene, *J. Biol. Chem.*, 1983, 258(23), 14120–14125. [https://doi.org/10.1016/S0021-9258\(17\)43831-2](https://doi.org/10.1016/S0021-9258(17)43831-2)
61. L. H. Fu, X. F. Wang, Y. Eyal, Y. M. She, L. J. Donald, K. G. Standing and G. Ben-Hayyim, A selenoprotein in the plant kingdom. Mass spectrometry confirms that an opal codon (UGA) encodes selenocysteine in *Chlamydomonas reinhardtii* glutathione peroxidase, *J. Biol. Chem.*, 2002, 277(29), 25983–25991. <https://doi.org/10.1074/jbc.M202912200>
62. V. M. Labunskyy, D. L. Hatfield and V. N. Gladyshev, Selenoproteins: molecular pathways and physiological roles, *Physiol. Rev.*, 2014, 94(3), 739–777. <https://doi.org/10.1152/physrev.00039.2013>
63. L. Flohe, W. A. Günzler and H. H. Schock, Glutathione peroxidase: a selenoenzyme, *FEBS Lett.*, 1973, 32(1), 132–134. [https://doi.org/10.1016/0014-5793\(73\)80755-0](https://doi.org/10.1016/0014-5793(73)80755-0)
64. J. E. Cone, R. M. Del Río, J. N. Davis and T. C. Stadtman, Chemical characterization of the selenoprotein component of clostridial glycine reductase: identification of selenocysteine as the organoselenium moiety, *Proc. Natl. Acad. Sci.*, 1976, 73(8), 2659–2663. <https://doi.org/10.1073/pnas.73.8.2659>
65. F. Zinoni, A. Birkmann, T. C. Stadtman and A. Böck, Nucleotide sequence and expression of the selenocysteine-containing polypeptide of formate dehydrogenase (formate-hydrogen-lyase-linked) from *Escherichia coli*, *Proc. Natl. Acad. Sci.*, 1986, 83(13), 4650–4654. <https://doi.org/10.1073/pnas.83.13.4650>
66. I. Chambers, J. Frampton, P. Goldfarb, N. Affara, W. McBain and P. R. Harrison, The structure of the mouse glutathione peroxidase gene: the selenocysteine in the active site is encoded by the ‘termination’ codon, TGA, *EMBO J.*, 1986, 5(6), 1221–1227. <https://doi.org/10.1002/j.1460-2075.1986.tb04350.x>
67. D. Rehder, The role of vanadium in biology, *Metallomics*, 2015, 7(5), 730–742. <https://doi.org/10.1039/c4mt00304g>

68. M. Weyand, H. J. Hecht, M. Kieß, M. F. Liaud, H. Vilter and D. Schomburg, X-ray structure determination of a vanadium-dependent haloperoxidase from *Ascophyllum nodosum* at 2.0 Å resolution, *J. Mol. Biol.*, 1999, 293(3), 595–611. <https://doi.org/10.1006/jmbi.1999.3179>
69. H. Vilter, Peroxidases from phaeophyceae: a vanadium(V)-dependent peroxidase from *Ascophyllum nodosum*, *Phytochemistry*, 1984, 23(7), 1387–1390. [https://doi.org/10.1016/S0031-9422\(00\)80471-9](https://doi.org/10.1016/S0031-9422(00)80471-9)
70. R. L. Robson, R. R. Eady, T. H. Richardson, R. W. Miller, M. Hawkins and J. R. Postgate, The alternative nitrogenase of *Azotobacter chroococcum* is a vanadium enzyme, *Nature*, 1986, 322(6077), 388–390. <https://doi.org/10.1038/322388a0>
71. S. J. Crockford, Evolutionary roots of iodine and thyroid hormones in cell–cell signaling, *Integr. Comp. Biol.*, 2009, 49(2), 155–166. <https://doi.org/10.1093/icb/icmp053>
72. F. C. Küpper and C. J. Carrano, Key aspects of the iodine metabolism in brown algae: a brief critical review, *Metallomics*, 2019, 11(4), 756–764. <https://doi.org/10.1039/c8mt00327k>
73. F. C. Küpper, L. J. Carpenter, G. B. McFiggans, C. J. Palmer, T. J. Waite, E.-M. Boneberg, S. Woitsch, M. Weiller, R. Abela, D. Grolimund, P. Potin, A. Butler, G. W. Luther, P. M. H. Kroneck, W. Meyer-Klaucke and M. C. Feiters, Iodide accumulation provides help with an inorganic antioxidant impacting atmospheric chemistry, *Proc. Natl. Acad. Sci.*, 2008, 105(19), 6954–6958. <https://doi.org/10.1073/pnas.0709959105>
74. A. Cosse, P. Potin and C. Leblanc, Patterns of gene expression induced by oligoguluronates reveal conserved and environment-specific molecular defense responses in the brown alga *Laminaria digitata*, *New Phytol.*, 2009, 182(1), 239–250. <https://doi.org/10.1111/j.1469-8137.2008.02745.x>
75. R. R. Mendel and T. Kruse, Cell biology of molybdenum in plants and humans, *Biochim. Biophys. Acta*, 2012, 1823(9), 1568–1579. <https://doi.org/10.1016/j.bbamcr.2012.02.007>
76. Y. Zhang and V. N. Gladyshev, Molybdoproteomes and evolution of molybdenum utilization, *J. Mol. Biol.*, 2008, 379(4), 881–899. <https://doi.org/10.1016/j.jmb.2008.03.051>
77. H. Bortels, Molybdän als katalysator bei der biologischen stickstoffbindung, *Arch. Mikrobiol.*, 1930, 1(1), 333–342. <https://doi.org/10.1007/BF00510471>
78. D. B. Zamble, Nickel in biology, *Metallomics*, 2015, 7(4), 588–589. <https://doi.org/10.1039/c5mt90013a>
79. G. Schwarz, R. R. Mendel and M. W. Ribbe, Molybdenum cofactors, enzymes and pathways, *Nature*, 2009, 460(7257), 839–847. <https://doi.org/10.1038/nature08302>
80. H. Fenton, On a new reaction of tartaric acid, *Chem News*, 1876, 33(190), 190.
81. R. P. Cunningham, H. Asahara, J. F. Bank, C. P. Scholes, J. C. Salerno, K. Surerus, E. Munck, J. McCracken, J. Peisach and M. H. Emptage, Endonuclease III is an iron-sulfur protein, *Biochemistry*, 1989, 28(10), 4450–4455. <https://doi.org/10.1021/bi00436a049>
82. J. C. Kendrew, R. E. Dickerson, B. E. Strandberg, R. G. Hart, D. R. Davies, D. C. Phillips and V. C. Shore, Structure of myoglobin: a three-dimensional fourier synthesis at 2 Å. Resolution, *Nature*, 1960, 185(4711), 422–427. <https://doi.org/10.1038/185422a0>
83. P. L. Roach, I. J. Clifton, C. M. H. Hensgens, N. Shibata, C. J. Schofield, J. Hajdu and J. E. Baldwin, Structure of isopenicillin N synthase complexed with substrate and the mechanism of penicillin formation, *Nature*, 1997, 387(6635), 827–830. <https://doi.org/10.1038/42990>
84. D. J. Netz, C. M. Stith, M. Stümpfig, G. Köpf, D. Vogel, H. M. Genau, J. L. Stodola, R. Lill, P. M. Burgers and A. J. Pierik, Eukaryotic DNA polymerases require an iron-sulfur cluster for the formation of active complexes, *Nat. Chem. Biol.*, 2011, 8(1), 125–132. <https://doi.org/10.1038/nchembio.721>
85. A. H. Robbins and C. D. Stout, The structure of aconitase, *Proteins Struct. Funct. Bioinf.*, 1989, 5(4), 289–312. <https://doi.org/10.1002/prot.340050406>
86. B. K. Vainshtein, W. R. Melik-Adamyanyan, V. V. Barynin, A. A. Vagin and A. I. Grebenko, Three-dimensional structure of the enzyme catalase, *Nature*, 1981, 293(5831), 411–412. <https://doi.org/10.1038/293411a0>
87. S. Iwata, C. Ostermeier, B. Ludwig and H. Michel, Structure at 2.8 Å resolution of cytochrome c oxidase from *Paracoccus denitrificans*, *Nature*, 1995, 376(6542), 660–669. <https://doi.org/10.1038/376660a0>
88. T. Tsukihara, H. Aoyama, E. Yamashita, T. Tomizaki, H. Yamaguchi, K. Shinzawa-Itoh, R. Nakashima, R. Yaono and S. Yoshikawa, Structures of metal sites of oxidized bovine heart cytochrome c oxidase at 2.8 Å, *Science*, 1995, 269(5227), 1069–1074. <https://doi.org/10.1126/science.7652554>
89. M. E. Cuff, K. I. Miller, K. E. van Holde and W. A. Hendrickson, Crystal structure of a functional unit from *Octopus hemocyanin*, *J. Mol. Biol.*, 1998, 278(4), 855–870. <https://doi.org/10.1006/jmbi.1998.1647>
90. M. J. Boulanger and M. E. P. Murphy, Alternate substrate binding modes to two mutant (D98N and H255N) forms of nitrite reductase from *Alcaligenes faecalis* S-6: structural model of a transient catalytic intermediate, *Biochemistry*, 2001, 40(31), 9132–9141. <https://doi.org/10.1021/bi0107400>
91. J. A. Tainer, E. D. Getzoff, J. S. Richardson and D. C. Richardson, Structure and mechanism of copper, zinc superoxide dismutase, *Nature*, 1983, 306(5940), 284–287. <https://doi.org/10.1038/306284a0>
92. S. Dzul, T. L. Stemmler and J. E. Penner-Hahn, Manganese proteins with mono- and dinuclear metal sites, In: RA Scott (ed.), *Encyclopedia of Inorganic and Bioinorganic Chemistry*, Wiley, Hoboken, NJ, 2015, pp. 1–11.
93. G. E. O. Borgstahl, H. E. Parge, M. J. Hickey, W. F. Beyer, Jr, R. A. Hallewell and J. A. Tainer, The structure of human mitochondrial manganese superoxide dismutase reveals a novel tetrameric interface of two 4-helix bundles, *Cell*, 1992, 71(1), 107–118. [https://doi.org/10.1016/0092-8674\(92\)90270-M](https://doi.org/10.1016/0092-8674(92)90270-M)
94. N. Cox, H. Ogata, P. Stolle, E. Reijerse, G. Auling and W. Lubitz, A tyrosyl–dimanganese coupled spin system is the native metalloradical cofactor of the R2F subunit of the ribonucleotide reductase of *Corynebacterium ammoniagenes*, *J. Am. Chem. Soc.*, 2010, 132(32), 11197–11213. <https://doi.org/10.1021/ja1036995>
95. M. J. Jedrzejas, M. Chander, P. Setlow and G. Krishnasamy, Structure and mechanism of action of a novel phosphoglycerate mutase from *Bacillus stearothermophilus*, *EMBO J.*, 2000, 19(7), 1419–1431. <https://doi.org/10.1093/emboj/19.7.1419>
96. I. Yruela, Transition metals in plant photosynthesis, *Metallomics*, 2013, 5(9), 1090–1109. <https://doi.org/10.1039/c3mt00086a>
97. J. Przybyla-Toscano, C. Boussardon, S. R. Law, N. Rouhier and O. Keech, Gene atlas of iron-containing proteins in *Arabidopsis thaliana*, *Plant J.*, 2021, 106(1), 258–274. <https://doi.org/10.1111/tbj.15154>

98. R. P. Hausinger, Metallocenter assembly in nickel-containing enzymes, *JBIC J. Biol. Inorg. Chem.*, 1997, 2(3), 279–286. <https://doi.org/10.1007/s007750050133>
99. M. Kobayashi and S. Shimizu, Cobalt proteins, *Eur. J. Biochem.*, 1999, 261(1), 1–9. <https://doi.org/10.1046/j.1432-1327.1999.00186.x>
100. C. L. Drennan, S. Huang, J. T. Drummond, R. G. Matthews and M. L. Ludwig, How a protein binds B12: a 3.0 Å X-ray structure of B12-binding domains of methionine synthase, *Science*, 1994, 266(5191), 1669–1674. <https://doi.org/10.1126/science.7992050>
101. R. Hille, T. Nishino and F. Bittner, Molybdenum enzymes in higher organisms, *Coord. Chem. Rev.*, 2011, 255(9–10), 1179–1205. <https://doi.org/10.1016/j.ccr.2010.11.034>
102. C. Enroth, B. T. Eger, K. Okamoto, T. Nishino, T. Nishino and E. F. Pai, Crystal structures of bovine milk xanthine dehydrogenase and xanthine oxidase: structure-based mechanism of conversion, *Proc. Natl. Acad. Sci.*, 2000, 97(20), 10723–10728. <https://doi.org/10.1073/pnas.97.20.10723>
103. C. Kisker, H. Schindelin, A. Pacheco, W. A. Wehbi, R. M. Garrett, K. V. Rajagopalan, J. H. Enemark and D. C. Rees, Molecular basis of sulfite oxidase deficiency from the structure of sulfite oxidase, *Cell*, 1997, 91(7), 973–983. [https://doi.org/10.1016/S0092-8674\(00\)80488-2](https://doi.org/10.1016/S0092-8674(00)80488-2)
104. P. I. Oteiza, Zinc and the modulation of redox homeostasis, *Free Radic. Biol. Med.*, 2012, 53(9), 1748–1759. <https://doi.org/10.1016/j.freeradbiomed.2012.08.568>
105. A. Sharma, B. Patni, D. Shankhdhar and S. C. Shankhdhar, Zinc—an indispensable micronutrient, *Physiol. Mol. Biol. Plants*, 2013, 19(1), 11–20. <https://doi.org/10.1007/s12298-012-0139-1>
106. C. M. Palmer and M. L. Guerinot, Facing the challenges of Cu, Fe and Zn homeostasis in plants, *Nat. Chem. Biol.*, 2009, 5(5), 333–340. <https://doi.org/10.1038/nchembio.166>
107. M. Gupta and S. Gupta, An overview of selenium uptake, metabolism, and toxicity in plants, *Front. Plant Sci.*, 2016, 7(2074), 2074. <https://doi.org/10.3389/fpls.2016.02074>
108. H. J. Reich and R. J. Hondal, Why nature chose selenium, *ACS Chem. Biol.*, 2016, 11(4), 821–841. <https://doi.org/10.1021/acschembio.6b00031>
109. J. E. Cone, R. M. Del Río, J. N. Davis and T. C. Stadtman, Chemical characterization of the selenoprotein component of clostridial glycine reductase: identification of selenocysteine as the organoselenium moiety, *Proc. Natl. Acad. Sci. USA*, 1976, 73(8), 2659–2663. <https://doi.org/10.1073/pnas.73.8.2659>
110. N. Yurkova, N. Saveleva and N. Lyalikova, Oxidation of molecular-hydrogen and carbon-monoxide by facultatively chemolithotrophic vanadate-reducing bacteria, *Microbiology*, 1993, 62(4), 367–370.
111. W. Carpentier, K. Sandra, I. De Smet, A. Brigé, L. De Smet and J. Van Beeumen, Microbial reduction and precipitation of vanadium by *Shewanella oneidensis*, *Appl. Environ. Microbiol.*, 2003, 69(6), 3636–3639. <https://doi.org/10.1128/aem.69.6.3636-3639.2003>
112. I. Uluisik, H. C. Karakaya and A. Koc, The importance of boron in biological systems, *J. Trace Elem. Med. Biol.*, 2018, 45, 156–162. <https://doi.org/10.1016/j.jtemb.2017.10.008>
113. R. Hutter, W. Keller-Schierlein, F. Knusel, V. Prelog, G. C. Rodgers, Jr, P. Suter, G. Vogel, W. Voser and H. Zahner, The metabolic products of microorganisms. Boromycin, *Helv. Chim. Acta*, 1967, 50(6), 1533–1539. <https://doi.org/10.1002/hlca.19670500612>
114. M. Kobayashi, T. Matoh and J. Azuma, Two chains of rhamnogalacturonan II are cross-linked by borate–diol ester bonds in higher plant cell walls, *Plant Physiol.*, 1996, 110(3), 1017–1020. <https://doi.org/10.1104/pp.110.3.1017>
115. A. Bennett, R. I. Rowe, N. Soch and C. D. Eckhart, Boron stimulates yeast (*Saccharomyces cerevisiae*) growth, *J. Nutr.*, 1999, 129(12), 2236–2238
116. D. H. Lewis, Boron: the essential element for vascular plants that never was, *New Phytol.*, 2019, 221(4), 1685–1690. <https://doi.org/10.1111/nph.15519>
117. A. Nozawa, J. Takano, M. Kobayashi, N. Von Wirén and T. Fujiwara, Roles of BOR1, DUR3, and FPS1 in boron transport and tolerance in *Saccharomyces cerevisiae*, *FEMS Microbiol. Lett.*, 2006, 262(2), 216–222. <https://doi.org/10.1111/j.1574-6968.2006.00395.x>
118. J. F. Ma and N. Yamaji, A cooperative system of silicon transport in plants, *Trends Plant Sci.*, 2015, 20(7), 435–442. <https://doi.org/10.1016/j.tplants.2015.04.007>
119. M. Hildebrand, B. E. Volcani, W. Gassmann and J. I. Schroeder, A gene family of silicon transporters, *Nature*, 1997, 385(6618), 688–689. <https://doi.org/10.1038/385688b0>
120. E. Rogall, Über den Feinbau der Kieselmembran der Diatomeen, *Planta*, 1939, 29(2), 279–291.
121. M. Pančić, R. R. Torres, R. Almeda and T. Kiørboe, Silicified cell walls as a defensive trait in diatoms, *Proc. R. Soc. B: Biol. Sci.*, 2019, 286(1901), 20190184. <https://doi.org/10.1098/rspb.2019.0184>
122. V. M. Dembitsky and D. O. Levitsky, Arsenolipids, *Prog. Lipid Res.*, 2004, 43(5), 403–448. <https://doi.org/10.1016/j.plipres.2004.07.001>
123. G. Lunde, Analysis of trace elements in seaweed, *J. Sci. Food Agric.*, 1970, 21(8), 416–418. <https://doi.org/10.1002/jsfa.2740210806>
124. Á. H. Pétursdóttir, K. Fletcher, H. Gunnlaugsdóttir, E. Krupp, F. C. Küpper and J. Feldmann, Environmental effects on arsenosugars and arsenolipids in *Ectocarpus* (Phaeophyta), *Environ. Chem.*, 2016, 13(1), 21–33. <https://doi.org/10.1071/en14229>
125. J. S. Martinez, G. L. Carroll, R. A. Tschirret-Guth, G. Altenhoff, R. D. Little and A. Butler, On the regioselectivity of vanadium bromoperoxidase, *J. Am. Chem. Soc.*, 2001, 123(14), 3289–3294. <https://doi.org/10.1021/ja004176c>
126. G. W. Gribble, The diversity of naturally occurring organobromine compounds, *Chem. Soc. Rev.*, 1999, 28(5), 335–346. <https://doi.org/10.1039/a900201d>
127. X. J. Duan, X. M. Li and B. G. Wang, Highly brominated mono- and bis-phenols from the marine red alga *Symphocladia latiuscula* with radical-scavenging activity, *J. Nat. Prod.*, 2007, 70(7), 1210–1213. <https://doi.org/10.1021/np070061b>
128. N. P. Hughes, C. C. Perry, O. R. Anderson and R. J. P. Williams, Biological minerals formed from strontium and barium sulphates. III. The morphology and crystallography of strontium sulphate crystals from the colonial radiolarian, *Sphaerozoum punctatum*, *Proc. R. Soc. Lond. B: Biol. Sci.*, 1997, 238(1292), 223–233. <https://doi.org/10.1098/rspb.1989.0078>
129. J. Decelle, P. Martin, K. Paborstava, D. W. Pond, G. Tarling, F. Mahé, C. de Vargas, R. Lampitt and N. F. Diversity, Ecology and biogeochemistry of cyst-forming Acantharia (Radiolaria) in the oceans, *PLoS One*, 2013, 8(1), e53598. <https://doi.org/10.1371/journal.pone.0053598>
130. M. M. Brisbin, O. D. Brunner, M. M. Grossmann and S. Mitarai, Paired high-throughput, in situ imaging and high-throughput sequencing illuminate acantharian abundance and vertical

- distribution, *Limnol. Oceanogr.*, 2020, 65(12), 2953–2965. <https://doi.org/10.1002/lno.11567>
131. N. M. Price and F. M. M. Morel, Cadmium and cobalt substitution for zinc in a marine diatom, *Nature*, 1990, 344(6267), 658–660. <https://doi.org/10.1038/344658a0>
 132. V. Alterio, E. Langella, F. Viparelli, D. Vullo, G. Ascione, N. A. Dathan, F. M. Morel, C. T. Supuran, G. De Simone and S. M. Monti, Structural and inhibition insights into carbonic anhydrase CDCA1 from the marine diatom *Thalassiosira weissflogii*, *Biochimie*, 2012, 94(5), 1232–1241. <https://doi.org/10.1016/j.biochi.2012.02.013>
 133. Y. Xu, L. Feng, P. D. Jeffrey, Y. Shi and F. M. M. Morel, Structure and metal exchange in the cadmium carbonic anhydrase of marine diatoms, *Nature*, 2008, 452(7183), 56–61. <https://doi.org/10.1038/nature06636>
 134. H. Park, B. Song and F. M. M. Morel, Diversity of the cadmium-containing carbonic anhydrase in marine diatoms and natural waters, *Environ. Microbiol.*, 2007, 9(2), 403–413. <https://doi.org/10.1111/j.1462-2920.2006.01151.x>
 135. Y. Hu, S. Faham, R. Roy, M. W. Adams and D. C. Rees, Formaldehyde ferredoxin oxidoreductase from *Pyrococcus furiosus*: the 1.85 Å resolution crystal structure and its mechanistic implications, *J. Mol. Biol.*, 1999, 286(3), 899–914. <https://doi.org/10.1006/jmbi.1998.2488>
 136. L. B. Maia, I. Moura and J. J. G. Moura, Molybdenum and tungsten-containing enzymes: an overview, In: R. Hille, C. Schulzke M Kirk (eds), *Molybdenum and Tungsten Enzymes: Biochemistry*, The Royal Society of Chemistry, 2017, ch. 1, pp. 1–80.
 137. I. Yamamoto, T. Saiki, S. M. Liu and L. G. Ljungdahl, Purification and properties of NADP-dependent formate dehydrogenase from *Clostridium thermoaceticum*, a tungsten-selenium-iron protein, *J. Biol. Chem.*, 1983, 258(3), 1826–1832. [https://doi.org/10.1016/S0021-9258\(18\)33062-X](https://doi.org/10.1016/S0021-9258(18)33062-X)
 138. M. K. Johnson, D. C. Rees and M. W. W. Adams, Tungstenoenzymes, *Chem. Rev.*, 1996, 96(7), 2817–2840. <https://doi.org/10.1021/cr950063d>
 139. B. M. Rosner and B. Schink, Purification and characterization of acetylene hydratase of *Pelobacter acetylenicus*, a tungsten iron-sulfur protein, *J. Bacteriol.*, 1995, 177(20), 5767–5772. <https://doi.org/10.1128/jb.177.20.5767-5772.1995>
 140. S. Lyu, X. Wei, J. Chen, C. Wang, X. Wang and D. Pan, Titanium as a beneficial element for crop production, *Front. Plant Sci.*, 2017, 8(597), 597. <https://doi.org/10.3389/fpls.2017.00597>
 141. D. S. Grégoire and A. J. Poulain, A physiological role for HgII during phototrophic growth, *Nat. Geosci.*, 2016, 9(2), 121–125. <https://doi.org/10.1038/ngeo2629>
 142. T. Barkay and I. Wagner-Döbler, Microbial transformations of mercury: potentials, challenges, and achievements in controlling mercury toxicity in the environment, *Adv. Appl. Microbiol.*, 2005, 57, 1–52.
 143. D. Ben-Bassat and A. M. Mayer, Volatilization of mercury by algae, *Physiol. Plant.*, 1975, 33(2), 128–132. <https://doi.org/10.1111/j.1399-3054.1975.tb03779.x>
 144. N. C. Martinez-Gomez, H. N. Vu and E. Skovran, Lanthanide chemistry: from coordination in chemical complexes shaping our technology to coordination in enzymes shaping bacterial metabolism, *Inorg. Chem.*, 2016, 55(20), 10083–10089. <https://doi.org/10.1021/acs.inorgchem.6b00919>
 145. J. A. Cotruvo, Jr, The chemistry of lanthanides in biology: recent discoveries, emerging principles, and technological applications, *ACS Cent. Sci.*, 2019, 5(9), 1496–1506. <https://doi.org/10.1021/acscentsci.9b00642>
 146. Y. Hibi, K. Asai, H. Arafuka, M. Hamajima, T. Iwama and K. Kawai, Molecular structure of La³⁺-induced methanol dehydrogenase-like protein in *Methylobacterium radiotolerans*, *J. Biosci. Bioeng.*, 2011, 111(5), 547–549. <https://doi.org/10.1016/j.jbiosc.2010.12.017>
 147. J. A. Cotruvo, Jr, E. R. Featherston, J. A. Mattocks, J. V. Ho and T. N. Laremore, Lanmodulin: a highly selective lanthanide-binding protein from a lanthanide-utilizing bacterium, *J. Am. Chem. Soc.*, 2018, 140(44), 15056–15061. <https://doi.org/10.1021/jacs.8b09842>
 148. J. A. Bogart, A. J. Lewis and E. J. Schelter, DFT study of the active site of the XoxF-type natural, cerium-dependent methanol dehydrogenase enzyme, *Chemistry*, 2015, 21(4), 1743–1748. <https://doi.org/10.1002/chem.201405159>
 149. N. A. Fitriyanto, M. Fushimi, M. Matsunaga, A. Pertiwinigrum, T. Iwama and K. Kawai, Molecular structure and gene analysis of Ce³⁺-induced methanol dehydrogenase of *Bradyrhizobium* sp. MAFF211645, *J. Biosci. Bioeng.*, 2011, 111(6), 613–617. <https://doi.org/10.1016/j.jbiosc.2011.01.015>
 150. A. Pol, T. R. M. Barends, A. Dietl, A. F. Khadem, J. Eygensteyn and M. S. M. Jetten, Op den Camp HJM. Rare earth metals are essential for methanotrophic life in volcanic mudpots, *Environ. Microbiol.*, 2014, 16(1), 255–264. <https://doi.org/10.1111/1462-2920.12249>
 151. J. A. Mattocks, J. V. Ho, J. A. Cotruvo, Jr and A. Selective, Protein-based fluorescent sensor with picomolar affinity for rare earth elements, *J. Am. Chem. Soc.*, 2019, 141(7), 2857–2861. <https://doi.org/10.1021/jacs.8b12155>
 152. A. Schmitz Rob, N. Picone, H. Singer, A. Dietl, K.-A. Seifert, A. Pol, S. M. Jetten Mike, R. M. Barends Thomas, J. Daumann Lena and H. J. M. Op den Camp, Neodymium as metal cofactor for biological methanol oxidation: structure and kinetics of an XoxF1-type methanol dehydrogenase, *mBio*, 2021, 12(5), e01708–e01721. <https://doi.org/10.1128/mBio.01708-21>
 153. L. A. Finney and T. V. O'Halloran, Transition metal speciation in the cell: insights from the chemistry of metal ion receptors, *Science*, 2003, 300(5621), 931–936. <https://doi.org/10.1126/science.1085049>
 154. J. A. Imlay, The mismetallation of enzymes during oxidative stress, *J. Biol. Chem.*, 2014, 289(41), 28121–28128. <https://doi.org/10.1074/jbc.R114.588814>
 155. M. S. Cyert and C. C. Philpott, Regulation of cation balance in *Saccharomyces cerevisiae*, *Genetics*, 2013, 193(3), 677–713. <https://doi.org/10.1534/genetics.112.147207>
 156. C. E. Blaby-Haas and S. S. Merchant, Regulating cellular trace metal economy in algae, *Curr. Opin. Plant Biol.*, 2017, 39, 88–96. <https://doi.org/10.1016/j.pbi.2017.06.005>
 157. T. Dudev and C. Lim, Competition among metal ions for protein binding sites: determinants of metal ion selectivity in proteins, *Chem. Rev.*, 2014, 114(1), 538–556. <https://doi.org/10.1021/cr4004665>
 158. A. W. Foster, D. Osman and N. J. Robinson, Metal preferences and metallation, *J. Biol. Chem.*, 2014, 289(41), 28095–28103. <https://doi.org/10.1074/jbc.R114.588145>
 159. J. A. Cotruvo, Jr and J. Stubbe, Metallation and mismetallation of iron and manganese proteins in vitro and in vivo: the class I ribonucleotide reductases as a case study, *Metallomics*, 2012, 4(10), 1020–1036. <https://doi.org/10.1039/c2mt20142a>
 160. J. A. Imlay, Cellular defenses against superoxide and hydrogen peroxide, *Annu. Rev. Biochem.*, 2008, 77, 755–776. <https://doi.org/10.1146/annurev.biochem.77.061606.161055>
 161. S. Tottey, K. J. Waldron, S. J. Firbank, B. Reale, C. Bessant, K. Sato, T. R. Cheek, J. Gray, M. J. Banfield, C. Dennison and N. J. Robinson,

- Protein-folding location can regulate manganese-binding versus copper- or zinc-binding, *Nature*, 2008, 455(7216), 1138–1142. <https://doi.org/10.1038/nature07340>
162. N. J. Robinson and D. R. Winge, Copper metallochaperones, *Annu. Rev. Biochem.*, 2010, 79(1), 537–562. <https://doi.org/10.1146/annurev-biochem-030409-143539>
 163. D. A. Capdevila, K. A. Edmonds and D. P. Giedroc, Metallochaperones and metalloregulation in bacteria, *Essays Biochem.*, 2017, 61(2), 177–200. <https://doi.org/10.1042/EBC20160076>
 164. C. L. Dupont, A. Butcher, R. E. Valas, P. E. Bourne and G. Caetano-Anolles, History of biological metal utilization inferred through phylogenomic analysis of protein structures, *Proc. Natl. Acad. Sci. USA*, 2010, 107(23), 10567–10572. <https://doi.org/10.1073/pnas.0912491107>
 165. W. L. Guo, H. Nazim, Z. S. Liang and D. F. Yang, Magnesium deficiency in plants: an urgent problem, *Crop J.*, 2016, 4(2), 83–91. <https://doi.org/10.1016/j.cj.2015.11.003>
 166. Z. C. Chen, W. T. Peng, J. Li and H. Liao, Functional dissection and transport mechanism of magnesium in plants, *Semin. Cell Dev. Biol.*, 2018, 74, 142–152. <https://doi.org/10.1016/j.semcdb.2017.08.005>
 167. N. Terry and G. Low, Leaf chlorophyll content and its relation to the intracellular-localization of iron, *J. Plant Nutr.*, 1982, 5(4-7), 301–310. <https://doi.org/10.1080/01904168209362959>
 168. A. F. López-Millán, D. Duy and K. Philippar, Chloroplast iron transport proteins—function and impact on plant physiology, *Front. Plant Sci.*, 2016, 7, 178. <https://doi.org/10.3389/fpls.2016.00178>
 169. S. Merchant and L. Bogorad, Regulation by copper of the expression of plastocyanin and cytochrome c552 in *Chlamydomonas reinhardi*, *Mol. Cell. Biol.*, 1986, 6(2), 462–469.
 170. S. Lindskog, Structure and mechanism of carbonic anhydrase, *Pharmacol. Ther.*, 1997, 74(1), 1–20. [https://doi.org/10.1016/S0163-7258\(96\)00198-2](https://doi.org/10.1016/S0163-7258(96)00198-2)
 171. H. Aigner, R. H. Wilson, A. Bracher, L. Calisse, J. Y. Bhat, F. U. Hartl and M. Hayer-Hartl, Plant RuBisCo assembly in *E. coli* with five chloroplast chaperones including BSD2, *Science*, 2017, 358(6368), 1272–1278. <https://doi.org/10.1126/science.aap9221>
 172. D. Staiger, Chemical strategies for iron acquisition in plants, *Angew. Chem. Int. Ed Engl.*, 2002, 41(13), 2259–2264. [https://doi.org/10.1002/1521-3773\(20020703\)41:13<2259::AID-ANIE2259>3.0.CO;2-I](https://doi.org/10.1002/1521-3773(20020703)41:13<2259::AID-ANIE2259>3.0.CO;2-I)
 173. J. A. Imlay, Iron-sulphur clusters and the problem with oxygen, *Mol. Microbiol.*, 2006, 59(4), 1073–1082. <https://doi.org/10.1111/j.1365-2958.2006.05028.x>
 174. F. M. M. Morel, R. J. M. Hudson and N. M. Price, Limitation of productivity by trace metals in the sea, *Limnol. Oceanogr.*, 1991, 36(8), 1742–1755. <https://doi.org/10.4319/lo.1991.36.8.1742>
 175. D. J. Kosman, Molecular mechanisms of iron uptake in fungi, *Mol. Microbiol.*, 2003, 47(5), 1185–1197. <https://doi.org/10.1046/j.1365-2958.2003.03368.x>
 176. G. Peers and N. M. Price, Copper-containing plastocyanin used for electron transport by an oceanic diatom, *Nature*, 2006, 441(7091), 341–344. <https://doi.org/10.1038/nature04630>
 177. J. Kropat, S. D. Gallaher, E. I. Urzica, S. S. Nakamoto, D. Strenkert, S. Tottey, A. Z. Mason and S. S. Merchant, Copper economy in *Chlamydomonas*: prioritized allocation and reallocation of copper to respiration vs. photosynthesis, *Proc. Natl. Acad. Sci. USA*, 2015, 112(9), 2644–2651. <https://doi.org/10.1073/pnas.1422492112>
 178. E. Masse and S. Gottesman, A small RNA regulates the expression of genes involved in iron metabolism in *Escherichia coli*, *Proc. Natl. Acad. Sci. USA*, 2002, 99(7), 4620–4625. <https://doi.org/10.1073/pnas.032066599>
 179. S. Puig, E. Askeland and D. J. Thiele, Coordinated remodeling of cellular metabolism during iron deficiency through targeted mRNA degradation, *Cell*, 2005, 120(1), 99–110. <https://doi.org/10.1016/j.cell.2004.11.032>
 180. A. M. Terauchi, G. Peers, M. C. Kobayashi, K. K. Niyogi and S. S. Merchant, Trophic status of *Chlamydomonas reinhardtii* influences the impact of iron deficiency on photosynthesis, *Photosynth. Res.*, 2010, 105(1), 39–49. <https://doi.org/10.1007/s11120-010-9562-8>
 181. X. Xie, W. Hu, X. Fan, H. Chen and M. Tang, Interactions between phosphorus, zinc, and iron homeostasis in nonmycorrhizal and mycorrhizal plants, *Front. Plant Sci.*, 2019, 10, 1172. <https://doi.org/10.3389/fpls.2019.01172>
 182. I. Cakmak and H. Marschner, Mechanism of phosphorus-induced zinc deficiency in cotton. I. Zinc deficiency-enhanced uptake rate of phosphorus, *Physiol. Plant.*, 1986, 68(3), 483–490. <https://doi.org/10.1111/j.1399-3054.1986.tb03386.x>
 183. H. S. Reed, Effects of zinc deficiency on phosphate metabolism of the tomato plant, *Am. J. Bot.*, 1946, 33(10), 778–784. <https://doi.org/10.1002/j.1537-2197.1946.tb12940.x>
 184. A. Hong-Hermesdorf, M. Miethke, S. D. Gallaher, J. Kropat, S. C. Dodani, J. Chan, D. Barupala, D. W. Domaille, D. I. Shirasaki, J. A. Loo, P. K. Weber, J. Pett-Ridge, T. L. Stemmler, C. J. Chang and S. S. Merchant, Subcellular metal imaging identifies dynamic sites of Cu accumulation in *Chlamydomonas*, *Nat. Chem. Biol.*, 2014, 10(12), 1034–1042. <https://doi.org/10.1038/nchembio.1662>
 185. D. Malasarn, J. Kropat, S. I. Hsieh, G. Finazzi, D. Casero, J. A. Loo, M. Pellegrini, F. A. Wollman and S. S. Merchant, Zinc deficiency impacts CO₂ assimilation and disrupts copper homeostasis in *Chlamydomonas reinhardtii*, *J. Biol. Chem.*, 2013, 288(15), 10672–10683. <https://doi.org/10.1074/jbc.M113.455105>
 186. R. Docampo, D. A. Scott, A. E. Vercesi and S. N. Moreno, Intracellular Ca²⁺ storage in acidocalcisomes of *Trypanosoma cruzi*, *Biochem. J.*, 1995, 310(3), 1005–1012. <https://doi.org/10.1042/bj3101005>
 187. S. C. Li and P. M. Kane, The yeast lysosome-like vacuole: endpoint and crossroads, *Biochim. Biophys. Acta*, 2009, 1793(4), 650–663. <https://doi.org/10.1016/j.bbamcr.2008.08.003>
 188. C. E. Blaby-Haas and S. S. Merchant, Lysosome-related organelles as mediators of metal homeostasis, *J. Biol. Chem.*, 2014, 289(41), 28129–28136. <https://doi.org/10.1074/jbc.R114.592618>
 189. X. Tan, K. Li, Z. Wang, K. Zhu and J. Cao, A review of plant vacuoles: formation, located proteins, and functions, *Plants*, 2019, 8(9), 327. <https://doi.org/10.3390/plants8090327>
 190. R. Docampo, The origin and evolution of the acidocalcisome and its interactions with other organelles, *Mol. Biochem. Parasitol.*, 2016, 209(1-2), 3–9. <https://doi.org/10.1016/j.molbiopara.2015.10.003>
 191. R. Docampo, W. de Souza, K. Miranda, P. Rohloff and S. N. Moreno, Acidocalcisomes—conserved from bacteria to man, *Nat. Rev. Microbiol.*, 2005, 3(3), 251–261. <https://doi.org/10.1038/nrmicro1097>
 192. A. E. Vercesi, S. N. Moreno and R. Docampo, Ca²⁺/H⁺ exchange in acidic vacuoles of *Trypanosoma brucei*, *Biochem J.*, 1994, 304(1), 227–233. <https://doi.org/10.1042/bj3040227>
 193. J. Deng, D. J. Vine, S. Chen, Q. Jin, Y. S. Nashed, T. Peterka, S. Vogt and C. Jacobsen, X-ray ptychographic and fluorescence microscopy of frozen-hydrated cells using continuous scanning, *Sci. Rep.*, 2017, 7(1), 445. <https://doi.org/10.1038/s41598-017-00569-y>

194. M. Tsednee, M. Castruita, P. A. Salomé, A. Sharma, B. E. Lewis, S. R. Schmollinger, D. Strenkert, K. Holbrook, M. S. Otegui, K. Khatua, S. Das, A. Datta, S. Chen, C. Ramon, M. Ralle, P. K. Weber, T. L. Stemmler, J. Pett-Ridge, B. M. Hoffman and S. S. Merchant, Manganese co-localizes with calcium and phosphorus in *Chlamydomonas* acidocalcisomes and is mobilized in manganese-deficient conditions, *J. Biol. Chem.*, 2019, 294(46), 17626–17641. <https://doi.org/10.1074/jbc.RA119.009130>
195. S. Schmollinger, S. Chen, D. Strenkert, C. Hui, M. Ralle and S. S. Merchant, Single-cell visualization and quantification of trace metals in *Chlamydomonas* lysosome-related organelles, *Proc. Natl. Acad. Sci. USA*, 2021, 118(16), e2026811118. <https://doi.org/10.1073/pnas.2026811118>
196. F. Penen, M. P. Isaure, D. Dobritzsch, I. Bertalan, H. Castillo-Michel, O. Proux, E. Gontier, P. Le Coustumer and D. Schaumlöffel, Pools of cadmium in *Chlamydomonas reinhardtii* revealed by chemical imaging and XAS spectroscopy, *Metallomics*, 2017, 9(7), 910–923. <https://doi.org/10.1039/c7mt00029d>
197. F. Penen, J. Malherbe, M. P. Isaure, D. Dobritzsch, I. Bertalan, E. Gontier, P. Le Coustumer and D. Schaumlöffel, Chemical bioimaging for the subcellular localization of trace elements by high contrast TEM, TEM/X-EDS, and NanoSIMS, *J. Trace Elem. Med. Biol.*, 2016, 37, 62–68. <https://doi.org/10.1016/j.jtemb.2016.04.014>
198. S. Thomine and G. Vert, Iron transport in plants: better be safe than sorry, *Curr. Opin. Plant Biol.*, 2013, 16(3), 322–327. <https://doi.org/10.1016/j.cbpa.2013.01.003>
199. A. M. Koorts and M. Viljoen, Ferritin and ferritin isoforms I: structure–function relationships, synthesis, degradation and secretion, *Arch. Physiol. Biochem.*, 2007, 113(1), 30–54. <https://doi.org/10.1080/13813450701318583>
200. E. C. Theil, Ferritin protein nanocages use ion channels, catalytic sites, and nucleation channels to manage iron/oxygen chemistry, *Curr. Opin. Chem. Biol.*, 2011, 15(2), 304–311. <https://doi.org/10.1016/j.cbpa.2011.01.004>
201. F. Penen, M. P. Isaure, D. Dobritzsch, H. Castillo-Michel, E. Gontier, P. Le Coustumer, J. Malherbe and D. Schaumlöffel, Pyrenoidal sequestration of cadmium impairs carbon dioxide fixation in a microalga, *Plant Cell Environ.*, 2020, 43(2), 479–495. <https://doi.org/10.1111/pce.13674>
202. H. Ali and E. Khan, What are heavy metals? Long-standing controversy over the scientific use of the term ‘heavy metals’ – proposal of a comprehensive definition, *Toxicol. Environ. Chem.*, 2018, 100(1), 6–19. <https://doi.org/10.1080/02772248.2017.1413652>
203. L. Järup, Hazards of heavy metal contamination, *Br. Med. Bull.*, 2003, 68(1), 167–182. <https://doi.org/10.1093/bmb/ldg032>
204. P. B. Tchounwou, C. G. Yedjou, A. K. Patlolla and D. J. Sutton, Heavy metal toxicity and the environment, In: A Luch (ed.), *Molecular, Clinical and Environmental Toxicology: Volume 3: Environmental Toxicology*, Springer, Basel, 2012, pp. 133–164.
205. H. Ali, E. Khan and I. Ilahi, Environmental chemistry and ecotoxicology of hazardous heavy metals: environmental persistence, toxicity, and bioaccumulation, *J. Chem.*, 2019, 2019, 6730305. <https://doi.org/10.1155/2019/6730305>
206. G. Rich and K. Cherry, *Hazardous Waste Treatment Technologies*, Pudvan Publishing Co, Northbrook, IL, 1987.
207. N. Ahalya, T. Ramachandra and R. Kanamadi, Biosorption of heavy metals, *Res. J. Chem. Environ.*, 2003, 7(4), 71–79.
208. R. J. Lawton, L. Mata, R. de Nys and N. A. Paul, Algal bioremediation of waste waters from land-based aquaculture using *Ulva*: selecting target species and strains, *PLoS One*, 2013, 8(10), e77344. <https://doi.org/10.1371/journal.pone.0077344>
209. M. Fabris, R. M. Abbriano, M. Pernice, D. L. Sutherland, A. S. Commault, C. C. Hall, L. Labeeuw, J. I. McCauley, U. Kuzhiuparambil, P. Ray, T. Kahlke and P. J. Ralph, Emerging technologies in algal biotechnology: toward the establishment of a sustainable, algae-based bioeconomy, *Front. Plant Sci.*, 2020, 11, 279. <https://doi.org/10.3389/fpls.2020.00279>
210. R. K. Goswami, K. Agrawal, M. P. Shah and P. Verma, Bioremediation of heavy metals from wastewater: a current perspective on microalgae-based future, *Lett. Appl. Microbiol.*, 2022, 75(4), 701–717. <https://doi.org/10.1111/lam.13564>
211. M. Garg, N. Sharma, S. Sharma, P. Kapoor, A. Kumar, V. Chunduri and P. Arora, Biofortified crops generated by breeding, agronomy, and transgenic approaches are improving lives of millions of people around the world, *Front. Nutr.*, 2018, 5, 12. <https://doi.org/10.3389/fnut.2018.00012>
212. M. Ferreira, P. C. Ribeiro, L. Ribeiro, M. Barata, V. F. Domingues, S. Sousa, C. Soares, A. Marques, P. Pousao-Ferreira, J. Dias, L. F. C. Castro, A. Marques, M. L. Nunes and L. M. P. Valente, Biofortified diets containing algae and selenised yeast: effects on growth performance, nutrient utilization, and tissue composition of gilthead seabream (*Sparus aurata*), *Front. Physiol.*, 2021, 12, 812884. <https://doi.org/10.3389/fphys.2021.812884>
213. T. Punshon, M. L. Guerinot and A. Lanzirrotti, Using synchrotron X-ray fluorescence microprobes in the study of metal homeostasis in plants, *Ann. Bot.*, 2009, 103(5), 665–672. <https://doi.org/10.1093/aob/mcn264>
214. C. M. Ackerman, S. Lee and C. J. Chang, Analytical methods for imaging metals in biology: from transition metal metabolism to transition metal signaling, *Anal. Chem.*, 2017, 89(1), 22–41. <https://doi.org/10.1021/acs.analchem.6b04631>
215. T. J. Stewart, Across the spectrum: integrating multidimensional metal analytics for in situ metallomic imaging, *Metallomics*, 2019, 11(1), 29–49. <https://doi.org/10.1039/c8mt00235e>
216. D. G. Schulze and P. M. Bertsch, Synchrotron X-ray techniques in soil, plant, and environmental research, In: DL Sparks (ed). *Advances in Agronomy*, Academic Press, Cambridge, MA, 1995, 1–66.
217. D. J. Hare, E. J. New, M. D. de Jonge and G. McColl, Imaging metals in biology: balancing sensitivity, selectivity and spatial resolution, *Chem. Soc. Rev.*, 2015, 44(17), 5941–5958. <https://doi.org/10.1039/c5cs00055f>
218. K. P. Carter, A. M. Young and A. E. Palmer, Fluorescent sensors for measuring metal ions in living systems, *Chem. Rev.*, 2014, 114(8), 4564–4601. <https://doi.org/10.1021/cr400546e>
219. B. J. McCranor, R. A. Bozym, M. I. Vitolo, C. A. Fierke, L. Bambrick, B. M. Polster, G. Fiskum and R. B. Thompson, Quantitative imaging of mitochondrial and cytosolic free zinc levels in an in vitro model of ischemia/reperfusion, *J. Bioenerg. Biomembr.*, 2012, 44(2), 253–263. <https://doi.org/10.1007/s10863-012-9427-2>
220. P. M. Kopittke, T. Punshon, D. J. Paterson, R. V. Tappero, P. Wang, F. P. C. Blamey, A. van der Ent and E. Lombi, Synchrotron-based X-ray fluorescence microscopy as a technique for imaging of elements in plants, *Plant Physiol.*, 2018, 178(2), 507–523. <https://doi.org/10.1104/pp.18.00759>
221. M. J. Pushie, I. J. Pickering, M. Korbas, M. J. Hackett and G. N. George, Elemental and chemically specific X-ray fluorescence imaging of biological systems, *Chem. Rev.*, 2014, 114(17), 8499–8541. <https://doi.org/10.1021/cr4007297>
222. U. E. A. Fittschen, H. H. Kunz, R. Höhner, I. M. B. Tyssebotn and A. Fittschen, A new micro X-ray fluorescence spectrometer for in vivo elemental analysis in plants, *X-Ray Spectrom.*, 2017, 46(5), 374–381. <https://doi.org/10.1002/xrs.2783>

223. S. Chen, J. Deng, Y. Yuan, C. Flachenecker, R. Mak, B. Hornberger, Q. Jin, D. Shu, B. Lai, J. Maser, C. Roehrig, T. Paunesku, S. C. Gleber, D. J. Vine, L. Finney, J. VonOsinski, M. Bolbat, I. Spink, Z. Chen, J. Steele, D. Trapp, J. Irwin, M. Feser, E. Snyder, K. Brister, C. Jacobsen, G. Woloschak and S. Vogt, The bionanoprobe: hard X-ray fluorescence nanoprobe with cryogenic capabilities, *J. Synchrotron Radiat.*, 2014, 21(1), 66–75. <https://doi.org/10.1107/S1600577513029676>
224. G. Martinez-Criado, J. Villanova, R. Tucoulou, D. Salomon, J. P. Suuronen, S. Laboure, C. Guilloud, V. Valls, R. Barrett, E. Gagliardini, Y. Dabin, R. Baker, S. Bohic, C. Cohen and J. Morse, ID16B: a hard X-ray nanoprobe beamline at the ESRF for nano-analysis, *J. Synchrotron Radiat.*, 2016, 23(1), 344–352. <https://doi.org/10.1107/S1600577515019839>
225. H. F. Yan, N. Bouet, J. Zhou, X. J. Huang, E. Nazaretski, W. H. Xu, A. P. Cocco, W. K. S. Chiu, K. S. Brinkman and Y. S. Chu, Multimodal hard x-ray imaging with resolution approaching 10 nm for studies in material science, *Nano Futures*, 2018, 2(1), 011001. <https://doi.org/Artn.01100110.1088/2399-1984/Aab25d>
226. S. Matsuyama, M. Shimura, M. Fujii, K. Maeshima, H. Yumoto, H. Mimura, Y. Sano, M. Yabashi, Y. Nishino, K. Tamasaku, Y. Ishizaka, T. Ishikawa and K. Yamauchi, Elemental mapping of frozen-hydrated cells with cryo-scanning X-ray fluorescence microscopy, *X-Ray Spectrom.*, 2010, 39(4), 260–266. <https://doi.org/10.1002/xrs.1256>
227. C. G. Schroer, P. Boye, J. M. Feldkamp, J. Patommel, D. Samberg, A. Schropp, A. Schwab, S. Stephan, G. Falkenberg, G. Wellenreuther and N. Reimers, Hard X-ray nanoprobe at beamline P06 at PETRA III, *Nucl. Instrum. Meth. A*, 2010, 616(2-3), 93–97. <https://doi.org/10.1016/j.nima.2009.10.094>
228. A. Somogyi, K. Medjoubi, G. Baranton, V. Le Roux, M. Ribbens, F. Polack, P. Philippot and J. P. Samama, Optical design and multi-length-scale scanning spectro-microscopy possibilities at the Nanoscopium beamline of Synchrotron Soleil, *J. Synchrotron Radiat.*, 2015, 22(4), 1118–1129. <https://doi.org/10.1107/S1600577515009364>
229. R. P. Winarski, M. V. Holt, V. Rose, P. Fuesz, D. Carbaugh, C. Benson, D. Shu, D. Kline, G. B. Stephenson, I. McNulty and J. Maser, A hard X-ray nanoprobe beamline for nanoscale microscopy, *J. Synchrotron Radiat.*, 2012, 19(6), 1056–1060. <https://doi.org/10.1107/S0909049512036783>
230. M. Cotte, E. Pouyet, M. Salomé, C. Rivard, W. De Nolf, H. Castillo-Michel, T. Fabris, L. Monico, K. Janssens, T. Wang, P. Sciau, L. Verger, L. Cormier, O. Dargaud, E. Brun, D. Bugnazet, B. Fayard, B. Hesse, A. E. Pradas del Real, G. Veronesi, J. Langlois, N. Balcar, Y. Vandenberghe, V. A. Solé, J. Kieffer, R. Barrett, C. Cohen, C. Cornu, R. Baker, E. Gagliardini, E. Papillon and J. Susini, The ID21 X-ray and infrared microscopy beamline at the ESRF: status and recent applications to artistic materials, *J. Anal. At. Spectrom.*, 2017, 32(3), 477–493. <https://doi.org/10.1039/c6ja00356g>
231. P. D. Quinn, L. Alianelli, M. Gomez-Gonzalez, D. Mahoney, F. Cacho-Nerin, A. Peach and J. E. Parker, The hard X-ray nanoprobe beamline at diamond light source, *J. Synchrotron Radiat.*, 2021, 28(3), 1006–1013. <https://doi.org/10.1107/S1600577521002502>
232. L. J. Gamble and C. R. Anderton, Secondary ion mass spectrometry imaging of tissues, cells, and microbial systems, *Micros Today*, 2016, 24(2), 24–31. <https://doi.org/10.1017/S1551929516000018>
233. J. Malherbe, F. Penen, M.-P. Isaure, J. Frank, G. Hause, D. Dobritsch, E. Gontier, F. Horr  ard, F. Hillion and D. Schauml  ffel, A new radio frequency plasma oxygen primary ion source on nano secondary ion mass spectrometry for improved lateral resolution and detection of electropositive elements at single cell level, *Anal. Chem.*, 2016, 88(14), 7130–7136. <https://doi.org/10.1021/acs.analchem.6b01153>
234. G. N. George, I. J. Pickering, M. J. Pushie, K. Nienaber, M. J. Hackett, I. Ascone, B. Hedman, K. O. Hodgson, J. B. Aitken, A. Levina, C. Glover and P. A. Lay, X-ray-induced photo-chemistry and X-ray absorption spectroscopy of biological samples, *J. Synchrotron Radiat.*, 2012, 19(6), 875–886. <https://doi.org/10.1107/S090904951203943X>
235. S. J. M. Van Malderen, T. Van Acker and F. Vanhaecke, Sub-micrometer nanosecond LA-ICP-MS imaging at pixel acquisition rates above 250 Hz via a low-dispersion setup, *Anal. Chem.*, 2020, 92(8), 5756–5764. <https://doi.org/10.1021/acs.analchem.9b05056>
236. J. Jim  nez-Lamana, J. Szpunar and R.   binski, New frontiers of metallomics: elemental and species-specific analysis and imaging of single cells, In: MAZ Arruda (ed.), *Metallomics: The Science of Biometals*, Springer International Publishing, Cham, 2018, pp. 245–270.
237. T. Friedl, N. Brinkmann and K. I. Mohr, Algae (Eukaryotic), In: J. Reintner V Thiel (eds), *Encyclopedia of Geobiology*, Springer, Dordrecht, 2011, 10–20.
238. J. D. Palmer, The symbiotic birth and spread of plastids: how many times and whodunit? *J. Phycol.*, 2003, 39(1), 4–12. <https://doi.org/10.1046/j.1529-8817.2003.02185.x>
239. P. J. Keeling, The number, speed, and impact of plastid endosymbioses in eukaryotic evolution, *Annu. Rev. Plant Biol.*, 2013, 64(1), 583–607. <https://doi.org/10.1146/annurev-arplant-050312-120144>
240. P. A. Salome and S. S. Merchant, A series of fortunate events: introducing *Chlamydomonas* as a reference organism, *Plant Cell*, 2019, 31(8), 1682–1707. <https://doi.org/10.1105/tpc.18.00952>
241. S. S. Merchant, S. E. Prochnik, O. Vallon, E. H. Harris, S. J. Karpowicz, G. B. Witman, A. Terry, A. Salamov, L. K. Fritz-Laylin, L. Mar  chal-Drouard, W. F. Marshall, L. H. Qu, D. R. Nelson, A. A. Sanderfoot, M. H. Spalding, V. V. Kapitonov, Q. Ren, P. Ferris, E. Lindquist, H. Shapiro, S. M. Lucas, J. Grimwood, J. Schmutz, P. Cardol, H. Cerutti, G. Chanfreau, C. L. Chen, V. Cognat, M. T. Croft, R. Dent, S. Dutcher, E. Fern  ndez, H. Fukuzawa, D. Gonz  lez-Ballester, D. Gonz  lez-Halphen, A. Hallmann, M. Hanikenne, M. Hippler, W. Inwood, K. Jabbari, M. Kalanon, R. Kuras, P. A. Lefebvre, S. D. Lemaire, A. V. Lobanov, M. Lohr, A. Manuell, I. Meier, L. Mets, M. Mittag, T. Mittelmeier, J. V. Moroney, J. Moseley, C. Napoli, A. M. Nedelcu, K. Niyogi, S. V. Novoselov, I. T. Paulsen, G. Pazour, S. Purton, J. P. Ral, D. M. Ria  o-Pach  n, W. Riekhof, L. Rymarquis, M. Schroda, D. Stern, J. Umen, R. Willows, N. Wilson, S. L. Zimmer, J. Allmer, J. Balk, K. Bisova, C. J. Chen, M. Elias, K. Gendler, C. Hauser, M. R. Lamb, H. Ledford, J. C. Long, J. Minagawa, M. D. Page, J. Pan, W. Pootakham, S. Roje, A. Rose, E. Stahlberg, A. M. Terauchi, P. Yang, S. Ball, C. Bowler, C. L. Dieckmann, V. N. Gladyshev, P. Green, R. Jorgensen, S. Mayfield, B. Mueller-Roeber, S. Rajamani, R. T. Sayre, P. Brokstein, I. Dubchak, D. Goodstein, L. Hornick, Y. W. Huang, J. Jhaveri, Y. Luo, D. Mart  nez, W. C. Ngau, B. Otilar, A. Poliakov, A. Porter, L. Szajkowski, G. Werner, K. Zhou, I. V. Grigoriev, D. S. Rokhsar and A. R. Grossman, The *Chlamydomonas* genome reveals the evolution of key animal and plant functions, *Science*, 2007, 318(5848), 245–250.
242. J. A. Gimpel, E. A. Specht, D. R. Georgianna and S. P. Mayfield, Advances in microalgae engineering and synthetic biology applications for biofuel production, *Curr. Opin. Chem. Biol.*, 2013, 17(3), 489–495. <https://doi.org/10.1016/j.cbpa.2013.03.038>

243. P. G. Stephenson, C. M. Moore, M. J. Terry, M. V. Zubkov and T. S. Bibby, Improving photosynthesis for algal biofuels: toward a green revolution, *Trends Biotechnol.*, 2011, 29(12), 615–623. <https://doi.org/10.1016/j.tibtech.2011.06.005>
244. M. Castruita, D. Casero, S. J. Karpowicz, J. Kropat, A. Vieler, S. I. Hsieh, W. Yan, S. Cokus, J. A. Loo, C. Benning, M. Pellegrini and S. S. Merchant, Systems biology approach in *Chlamydomonas* reveals connections between copper nutrition and multiple metabolic steps, *Plant Cell*, 2011, 23(4), 1273–1292. <https://doi.org/10.1105/tpc.111.084400>
245. E. I. Urzica, D. Casero, H. Yamasaki, S. I. Hsieh, L. N. Adler, S. J. Karpowicz, C. E. Blaby-Haas, S. G. Clarke, J. A. Loo, M. Pellegrini and S. S. Merchant, Systems and trans-system level analysis identifies conserved iron deficiency responses in the plant lineage, *Plant Cell*, 2012, 24(10), 3921–3948. <https://doi.org/10.1105/tpc.112.102491>
246. M. Aksoy, W. Pootakham and A. R. Grossman, Critical function of a *Chlamydomonas reinhardtii* putative polyphosphate polymerase subunit during nutrient deprivation, *Plant Cell*, 2014, 26(10), 4214–4229. <https://doi.org/10.1105/tpc.114.129270>
247. E. Fernandez and A. Galvan, Inorganic nitrogen assimilation in *Chlamydomonas*, *J. Exp. Bot.*, 2007, 58(9), 2279–2287. <https://doi.org/10.1093/jxb/erm106>
248. J. L. Moseley, D. Gonzalez-Ballester, W. Pootakham, S. Bailey and A. R. Grossman, Genetic interactions between regulators of *Chlamydomonas* phosphorus and sulfur deprivation responses, *Genetics*, 2009, 181(3), 889–905. <https://doi.org/10.1534/genetics.108.099382>
249. M. D. Page, M. D. Allen, J. Kropat, E. I. Urzica, S. J. Karpowicz, S. I. Hsieh, J. A. Loo and S. S. Merchant, Fe sparing and Fe recycling contribute to increased superoxide dismutase capacity in iron-starved *Chlamydomonas reinhardtii*, *Plant Cell*, 2012, 24(6), 2649–2665. <https://doi.org/10.1105/tpc.112.098962>
250. J. Moseley, J. Quinn, M. Eriksson and S. Merchant, The *Crd1* gene encodes a putative di-iron enzyme required for photosystem I accumulation in copper deficiency and hypoxia in *Chlamydomonas reinhardtii*, *EMBO J.*, 2000, 19(10), 2139–2151. <https://doi.org/10.1093/emboj/19.10.2139>
251. M. D. Allen, J. Kropat and S. S. Merchant, Regulation and localization of isoforms of the aerobic oxidative cyclase in *Chlamydomonas reinhardtii*, *Photochem. Photobiol.*, 2008, 84(6), 1336–1342. <https://doi.org/10.1111/j.1751-1097.2008.00440.x>
252. S. S. Merchant, The elements of plant micronutrients, *Plant Physiol.*, 2010, 154(2), 512–515. <https://doi.org/10.1104/pp.110.161810>
253. J. C. Long, F. Sommer, M. D. Allen, S. F. Lu and S. S. Merchant, FER1 and FER2 encoding two ferritin complexes in *Chlamydomonas reinhardtii* chloroplasts are regulated by iron, *Genetics*, 2008, 179(1), 137–147. <https://doi.org/10.1534/genetics.107.083824>
254. K. Komsic-Buchmann, L. Wostehoff and B. Becker, The contractile vacuole as a key regulator of cellular water flow in *Chlamydomonas reinhardtii*, *Eukaryot Cell*, 2014, 13(11), 1421–1430. <https://doi.org/10.1128/EC.00163-14>
255. D. M. Nelson, P. Tréguer, M. A. Brzezinski, A. Leynaert and B. Queguiner, Production and dissolution of biogenic silica in the ocean: revised global estimates, comparison with regional data and relationship to biogenic sedimentation, *Global Biogeochem. Cycles*, 1995, 9(3), 359–372. <https://doi.org/10.1029/95gb01070>
256. P. D. Chappell, L. P. Whitney, T. L. Haddock, S. Menden-Deuer, E. G. Roy, M. L. Wells and B. D. Jenkins, *Thalassiosira* spp. community composition shifts in response to chemical and physical forcing in the northeast Pacific Ocean, *Front. Microbiol.*, 2013, 4, 273. <https://doi.org/10.3389/fmicb.2013.00273>
257. E. F. Stoermer and M. L. Centric Diatoms, Centric diatoms, In: JD Wehr RG Sheath (eds), *Freshwater Algae of North America*. Academic Press, Burlington, 2003, pp. 559–594.
258. M. Hildebrand, S. J. L. Lerch and R. P. Shrestha, Understanding diatom cell wall silicification—moving forward, *Front. Mar. Sci.*, 2018, 5. <https://doi.org/10.3389/fmars.2018.00125>
259. E. V. Armbrust, J. A. Berges, C. Bowler, B. R. Green, D. Martinez, N. H. Putnam, S. Zhou, A. E. Allen, K. E. Apt, M. Bechner, M. A. Brzezinski, B. K. Chaal, A. Chiovitti, A. K. Davis, M. S. Demarest, J. C. Detter, T. Glavina, D. Goodstein, M. Z. Hadi, U. Hellsten, M. Hildebrand, B. D. Jenkins, J. Jurka, V. V. Kapitonov, N. Kroger, W. W. Lau, T. W. Lane, F. W. Larimer, J. C. Lippmeier, S. Lucas, M. Medina, A. Montsant, M. Obornik, M. S. Parker, B. Palenik, G. J. Pazour, P. M. Richardson, T. A. Rynearson, M. A. Saito, D. C. Schwartz, K. Thamtrakoln, K. Valentin, A. Vardi, F. P. Wilkerson and D. S. Rokhsar, The genome of the diatom *Thalassiosira pseudonana*: ecology, evolution, and metabolism, *Science*, 2004, 306(5693), 79–86. <https://doi.org/10.1126/science.1101156>
260. M. Lommer, M. Specht, A. S. Roy, L. Kraemer, R. Andreson, M. A. Gutowska, J. Wolf, S. V. Bergner, M. B. Schilhabel, U. C. Klostermeier, R. G. Beiko, P. Rosenstiel, M. Hippler and J. LaRoche, Genome and low-iron response of an oceanic diatom adapted to chronic iron limitation, *Genome Biol.*, 2012, 13(7), R66. <https://doi.org/10.1186/gb-2012-13-7-r66>
261. N. Poulsen, P. M. Chesley and N. Kröger, Molecular genetic manipulation of the diatom *Thalassiosira pseudonana* (Bacillariophyceae), *J. Phycol.*, 2006, 42(5), 1059–1065. <https://doi.org/10.1111/j.1529-8817.2006.00269.x>
262. A. Falciatore, R. Casotti, C. Leblanc, C. Abrescia and C. Bowler, Transformation of nonselectable reporter genes in marine diatoms, *Mar. Biotechnol.*, 1999, 1(3), 239–251. <https://doi.org/10.1007/pl00011773>
263. M. Sumper and E. Brunner, Silica biomineralization in diatoms: the model organism *Thalassiosira pseudonana*, *Chembiochem: Eur. J. Chem. Biol.*, 2008, 9(8), 1187–1194. <https://doi.org/10.1002/cbic.200700764>
264. A. Marchetti and N. Cassar, Diatom elemental and morphological changes in response to iron limitation: a brief review with potential paleoceanographic applications, *Geobiology*, 2009, 7(4), 419–431. <https://doi.org/10.1111/j.1472-4669.2009.00207.x>
265. J. H. Martin, R. M. Gordon and S. E. Fitzwater, The case for iron, *Limnol. Oceanogr.*, 1991, 36(8), 1793–1802. <https://doi.org/10.4319/lo.1991.36.8.1793>
266. A. Tsuda, S. Takeda, H. Saito, J. Nishioka, Y. Nojiri, I. Kudo, H. Kiyosawa, A. Shiimoto, K. Imai, T. Ono, A. Shimamoto, D. Tsumune, T. Yoshimura, T. Aono, A. Hinuma, M. Kinugasa, K. Suzuki, Y. Sohrin, Y. Noiri, H. Tani, Y. Deguchi, N. Tsurushima, H. Ogawa, K. Fukami, K. Kuma and T. Saino, A mesoscale iron enrichment in the western subarctic Pacific induces a large centric diatom bloom, *Science*, 2003, 300(5621), 958–961. <https://doi.org/10.1126/science.1082000>
267. P. Horowitz, Some experiences with x-ray and proton microscopes, *Ann. NY Acad. Sci.*, 1978, 306(1), 203–222. <https://doi.org/10.1111/j.1749-6632.1978.tb25650.x>
268. B. S. Twining, S. B. Baines, N. S. Fisher, J. Maser, S. Vogt, C. Jacobsen, A. Tovar-Sanchez and S. A. Sanudo-Wilhelmy, Quantifying trace elements in individual aquatic protist cells with a synchrotron X-ray fluorescence microprobe, *Anal. Chem.*, 2003, 75(15), 3806–3816. <https://doi.org/10.1021/ac034227z>
269. B. S. Twining, S. B. Baines, N. S. Fisher, C. Jacobsen and J. Maser, Quantification and localization of trace metals in natural

- plankton cells using a synchrotron X-ray fluorescence microprobe, *J. Phys. IV France*, 2003, 104, 435–438.
270. B. S. Twining, S. B. Baines, N. S. Fisher and M. R. Landry, Cellular iron contents of plankton during the Southern Ocean Iron Experiment (SOFEX), *Deep Sea Res. Pt I*, 2004, 51(12), 1827–1850. <https://doi.org/10.1016/j.dsr.2004.08.007>
 271. B. S. Twining, S. Rauschenberg, P. L. Morton and S. Vogt, Metal contents of phytoplankton and labile particulate material in the North Atlantic Ocean, *Prog. Oceanogr.*, 2015, 137(Part A), 261–283. <https://doi.org/10.1016/j.pocean.2015.07.001>
 272. M. S. Adams, C. T. Dillon, S. Vogt, B. Lai, J. Stauber and D. F. Jolley, Copper uptake, intracellular localization, and speciation in marine microalgae measured by synchrotron radiation X-ray fluorescence and absorption microspectroscopy, *Environ. Sci. Technol.*, 2016, 50(16), 8827–8839. <https://doi.org/10.1021/acs.est.6b00861>
 273. J. Nuester, S. Vogt and B. S. Twining, Localization of iron within centric diatoms of the genus *Thalassiosira*, *J. Phycol.*, 2012, 48(3), 626–634. <https://doi.org/10.1111/j.1529-8817.2012.01165.x>
 274. M. D. de Jonge, C. Holzner, S. B. Baines, B. S. Twining, K. Ignatyev, J. Diaz, D. L. Howard, D. Legnini, A. Miceli, I. McNulty, C. J. Jacobsen and S. Vogt, Quantitative 3D elemental microtomography of *Cyclotella meneghiniana* at 400-nm resolution, *Proc. Natl. Acad. Sci. USA*, 2010, 107(36), 15676–15680. <https://doi.org/10.1073/pnas.1001469107>
 275. J. Diaz, E. Ingall, S. Vogt, M. D. de Jonge, D. Paterson, C. Rau and J. A. Brandes, Characterization of phosphorus, calcium, iron, and other elements in organisms at sub-micron resolution using X-ray fluorescence spectromicroscopy, *Limnol. Oceanogr. Meth.*, 2009, 7(1), 42–51. <https://doi.org/10.4319/lom.2009.7.42>
 276. J. Deng, D. J. Vine, S. Chen, Y. S. Nashed, Q. Jin, N. W. Phillips, T. Peterka, R. Ross, S. Vogt and C. J. Jacobsen, Simultaneous cryo X-ray ptychographic and fluorescence microscopy of green algae, *Proc. Natl. Acad. Sci. USA*, 2015, 112(8), 2314–2319. <https://doi.org/10.1073/pnas.1413003112>
 277. J. Deng, Y. H. Lo, M. Gallagher-Jones, S. Chen, A. Pryor, Jr, Q. Jin, Y. P. Hong, Y. S. G. Nashed, S. Vogt, J. Miao and C. Jacobsen, Correlative 3D x-ray fluorescence and ptychographic tomography of frozen-hydrated green algae, *Sci. Adv.*, 2018, 4(11), eaau4548. <https://doi.org/10.1126/sciadv.aau4548>
 278. T. Leonardo, E. Farhi, A. M. Boisson, J. Vial, P. Cloetens, S. Bohic and C. Rivasseau, Determination of elemental distribution in green micro-algae using synchrotron radiation nano X-ray fluorescence (SR-nXRF) and electron microscopy techniques—subcellular localization and quantitative imaging of silver and cobalt uptake by *Coccomyxa actinabiotis*, *Metallomics*, 2014, 6(2), 316–329. <https://doi.org/10.1039/c3mt00281k>
 279. C. Bottini, M. Dapiaggi, E. Erba, G. Faucher and N. Rotiroti, High resolution spatial analyses of trace elements in coccoliths reveal new insights into element incorporation in coccolithophore calcite, *Sci. Rep.*, 2020, 10(1), 9825. <https://doi.org/10.1038/s41598-020-66503-x>
 280. T. Beuvier, I. Probert, L. Beaufort, B. Suchéras-Marx, Y. Chushkin, F. Zontone and A. Gibaud, X-ray nanotomography of coccolithophores reveals that coccolith mass and segment number correlate with grid size, *Nat. Commun.*, 2019, 10(1), 751. <https://doi.org/10.1038/s41467-019-08635-x>
 281. E. H. Harris, *The Chlamydomonas Sourcebook Second Edition Introduction to Chlamydomonas and Its Laboratory Use*, Elsevier, San Diego, CA, 2008.
 282. S. H. Hutner, L. Provasoli, A. Schatz and C. P. Haskins, Some approaches to the study of the role of metals in the metabolism of microorganisms, *Proc. Am. Philos. Soc.*, 1950, 94(2), 152–170.
 283. J. Kropat, A. Hong-Hermesdorf, D. Casero, P. Ent, M. Castruita, M. Pellegrini, S. S. Merchant and D. Malasarn, A revised mineral nutrient supplement increases biomass and growth rate in *Chlamydomonas reinhardtii*, *Plant J.*, 2011, 66(5), 770–780. <https://doi.org/10.1111/j.1365-313X.2011.04537.x>
 284. J. M. Quinn and S. Merchant, Copper-responsive gene expression during adaptation to copper deficiency, *Methods Enzymol.*, 1998, 297, 263–279.
 285. M. Stitt, W. Wirtz and H. W. Heldt, Metabolite levels during induction in the chloroplast and extrachloroplast compartments of spinach protoplasts, *Biochim. Biophys. Acta*, 1980, 593(1), 85–102. [https://doi.org/10.1016/0005-2728\(80\)90010-9](https://doi.org/10.1016/0005-2728(80)90010-9)
 286. M. Stitt, W. Wirtz and H. W. Heldt, Regulation of sucrose synthesis by cytoplasmic fructosebisphosphatase and sucrose phosphate synthase during photosynthesis in varying light and carbon dioxide, *Plant Physiol.*, 1983, 72(3), 767–774. <https://doi.org/10.1104/pp.72.3.767>
 287. Q. Jin, T. Paunesku, B. Lai, S.-C. Gleber, S. I. Chen, L. Finney, D. Vine, S. Vogt, G. Woloschak and C. Jacobsen, Preserving elemental content in adherent mammalian cells for analysis by synchrotron-based x-ray fluorescence microscopy, *J. Microsc.*, 2017, 265(1), 81–93. <https://doi.org/10.1111/jmi.12466>
 288. K. Ganio, S. James, D. Hare, B. Roberts and G. McColl, Accurate biometal quantification per individual *Caenorhabditis elegans*, *Analyst*, 2016, 141. <https://doi.org/10.1039/C5AN02544C>
 289. K. Jurowski, B. Buszewski and W. Piekoszewski, The analytical calibration in (bio)imaging/mapping of the metallic elements in biological samples—definitions, nomenclature and strategies: state of the art, *Talanta*, 2015, 131, 273–285. <https://doi.org/10.1016/j.talanta.2014.07.089>
 290. S. Chen, T. Paunesku, Y. Yuan, Q. Jin, B. Hornberger, C. Flache-necker, B. Lai, K. Brister, C. Jacobsen, G. Woloschak and S. Vogt, The bionanoprobe: synchrotron-based hard X-ray fluorescence microscopy for 2D/3D trace element mapping, *Microsc Today*, 2015, 23(3), 26–29. <https://doi.org/10.1017/S1551929515000401>
 291. D. Strenkert, S. Schmollinger, S. D. Gallaher, P. A. Salome, S. O. Purvine, C. D. Nicora, T. Mettler-Altmann, E. Soubeyrand, A. P. M. Weber, M. S. Lipton, G. J. Basset and S. S. Merchant, Multi-omics resolution of molecular events during a day in the life of *Chlamydomonas*, *Proc. Natl. Acad. Sci. USA*, 2019, 116(6), 2374–2383. <https://doi.org/10.1073/pnas.1815238116>
 292. J. M. Zones, I. K. Blaby, S. S. Merchant and J. G. Umen, High-resolution profiling of a synchronized diurnal transcriptome from *Chlamydomonas reinhardtii* reveals continuous cell and metabolic differentiation, *Plant Cell*, 2015, 27(10), 2743–2769. <https://doi.org/10.1105/tpc.15.00498>
 293. J. L. Spudich and R. Sager, Regulation of the *Chlamydomonas* cell cycle by light and dark, *J. Cell. Biol.*, 1980, 85(1), 136–145. <https://doi.org/10.1083/jcb.85.1.136>
 294. J. R. Kates and R. F. Jones, The control of gametic differentiation in liquid cultures of *Chlamydomonas*, *J. Cell. Comp. Physiol.*, 1964, 63(2), 157–164. <https://doi.org/10.1002/jcp.1030630204>
 295. S. M. Vogt, A set of software tools for analysis and visualization of 3D X-ray fluorescence data sets, *J. Phys. IV France*, 2003, 104, 635–638.
 296. V. A. Solé, E. Papillon, M. Cotte, P. Walter and J. Susini, A multiplatform code for the analysis of energy-dispersive X-ray fluorescence spectra, *Spectrochim. Acta Part B*, 2007, 62(1), 63–68. <https://doi.org/10.1016/j.sab.2006.12.002>

297. M. Cotte, T. Fabris, G. Agostini, D. Motta Meira, L. De Viguerie and V. A. Solé, Watching kinetic studies as chemical maps using open-source software, *Anal. Chem.*, 2016, 88(12), 6154–6160. <https://doi.org/10.1021/acs.analchem.5b04819>
298. T. Nietzold, B. M. West, M. Stuckelberger, B. Lai, S. Vogt and M. I. Bertoni, Quantifying X-ray fluorescence data using MAPS, *J. Vis. Exp.*, 2018, (132), 56042. <https://doi.org/10.3791/56042>
299. R. Docampo, Acidocalcisomes and polyphosphate granules, In: JM Shively (ed.), *Inclusions in Prokaryotes*. Springer, Berlin, 2006, 53–70.
300. C. Stock, H. K. Grønlien, R. D. Allen and Y. Naitoh, Osmoregulation in *Paramecium*: in situ ion gradients permit water to cascade through the cytosol to the contractile vacuole, *J. Cell Sci.*, 2002, 115(11), 2339–2348. <https://doi.org/10.1242/jcs.115.11.2339>
301. F. Xu, X. Wu, L. H. Jiang, H. Zhao and J. Pan, An organelle K⁺ channel is required for osmoregulation in *Chlamydomonas reinhardtii*, *J. Cell Sci.*, 2016, 129(15), 3008–3014. <https://doi.org/10.1242/jcs.188441>